

PAPER • OPEN ACCESS

## Integrated assessment of global climate, air pollution, and dietary, malnutrition and obesity health impacts of food production and consumption between 2014 and 2018

To cite this article: Christopher S Malley *et al* 2021 *Environ. Res. Commun.* **3** 075001

View the [article online](#) for updates and enhancements.

## Environmental Research Communications



## PAPER

## OPEN ACCESS

RECEIVED  
1 April 2021REVISED  
29 May 2021ACCEPTED FOR PUBLICATION  
14 June 2021PUBLISHED  
1 July 2021

Original content from this work may be used under the terms of the [Creative Commons Attribution 4.0 licence](#).

Any further distribution of this work must maintain attribution to the author(s) and the title of the work, journal citation and DOI.



# Integrated assessment of global climate, air pollution, and dietary, malnutrition and obesity health impacts of food production and consumption between 2014 and 2018

Christopher S Malley<sup>1,\*</sup>, W Kevin Hicks<sup>1</sup>, Johan C I Kulyenstierna<sup>1</sup>, Eleni Michalopoulou<sup>1</sup>, Amy Molotoks<sup>1</sup>, Jessica Slater<sup>1</sup>, Charles G Heaps<sup>2</sup>, Silvia Ulloa<sup>2</sup>, Jason Veysey<sup>2</sup>, Drew T Shindell<sup>3</sup>, Daven K Henze<sup>4</sup>, Omar Nawaz<sup>4</sup>, Susan C Anenberg<sup>5</sup>, Brian Mantlana<sup>6</sup> and Timothy P Robinson<sup>7</sup>

<sup>1</sup> Stockholm Environment Institute, Department of Environment and Geography, University of York, United Kingdom

<sup>2</sup> US Center, Stockholm Environment Institute, Somerville, MA, United States of America

<sup>3</sup> Nicholas School of the Environment, Duke University, Durham, NC, United States of America

<sup>4</sup> Department of Mechanical Engineering, University of Colorado, Boulder, CO, United States of America

<sup>5</sup> Milken Institute, School of Public Health, George Washington University, Washington D.C., United States of America

<sup>6</sup> Council for Scientific and Industrial Research, South Africa

<sup>7</sup> Food and Agriculture Organization of the United Nations, Rome, Italy

\* Author to whom any correspondence should be addressed.

E-mail: [chris.malley@york.ac.uk](mailto:chris.malley@york.ac.uk)

**Keywords:** agriculture, health, diet, air pollution, greenhouse gases

## Abstract

Agriculture accounts for approximately 10% of global greenhouse gas emissions and is simultaneously associated with impacts on human health through food consumption, and agricultural air pollutant emissions. These impacts are often quantified separately, and there is a lack of modelling tools to facilitate integrated assessments. This work presents a new model that integrates assessment of agricultural systems on (i) human health indirectly through dietary, obesity and malnutrition health risks from food consumption, (ii) human health directly through exposure to air pollutants from agricultural emissions, and (iii) greenhouse gas emissions. In the model, national food demand is the starting point from which the livestock and crop production systems that meet this are represented. The model is applied for 2014–2018 to assess the robustness of the GHG emissions and health burden results that this integrated modelling framework produces compared to previous studies that have quantified these variables independently. Methane and nitrous oxide emissions globally in 2018 were estimated to be 129 and 4.4 million tonnes, respectively, consistent with previous estimates. Agricultural systems were also estimated to emit 44 million tonnes of ammonia. An estimated 4.1 million deaths were associated with dietary health risks, 6.0 million with overweight/obesity, and 730 thousand infant deaths from malnutrition, consistent with previous studies. Agricultural air pollutant emissions were estimated to be associated with 537 thousand premature deaths attributable to fine particulate matter (PM<sub>2.5</sub>) exposure, and 184 thousand premature deaths from methane-induced ground-level ozone. These health impacts provide substantial opportunities to design integrated strategies that mitigate climate change, and improve human health, and also highlight possible trade-offs that the expansion of agricultural production could have due to increased emissions. The model presented here provides for the consistent evaluation of the implications of different agricultural strategies to meet food demand while minimising human health and climate change impacts.

## 1. Introduction

Agriculture contributes 10%–12% of global greenhouse gas (GHG) emissions, excluding land-use change Myhre *et al* (IPCC 2013). In national commitments to mitigate climate change, 89% of countries included the

agriculture sector as part of their mitigation component (FAO 2016). However, the majority did not elaborate on specific actions to achieve agricultural GHG emission reductions (FAO 2016). Therefore, as countries update their commitments, there is a substantial opportunity to clarify and strengthen climate change mitigation through an increased focus on mitigation actions to limit agricultural GHG emissions (Ross *et al* 2019). One approach to increasing climate change mitigation ambition is to link to key sustainable development goals (SDGs) (Linnér *et al* 2012, Shindell *et al* 2017). Food consumption and production are linked to a wide range of SDGs, including indirect impacts on human health through food consumption, e.g. from malnutrition, obesity, and dietary risk factors (Willett *et al* 2019, Zagnutt *et al* 2019), which relate to SDG 2: Zero Hunger and SDG 3: Good Health and Wellbeing, on human health from air pollutants from agricultural emissions (also SDG 3) (Lelieveld *et al* 2015), nitrogen pollution (Fowler *et al* 2015, San Martín 2020) and deforestation (IPCC 2019a), which relate to SDG 15: Life on Land.

Previous studies have modelled different impacts of food production and consumption individually. For example, Murray *et al* (2020) estimates global health impacts of malnutrition, high body-mass index, and dietary risk factors. Separately, Lelieveld *et al* (2015) estimated that 20% of global premature deaths (660 thousand premature deaths) attributable to ambient air pollution exposure were due to agriculture. However, methodological differences in the representation of agricultural systems make direct comparisons of the impacts quantified challenging. Other studies have developed models that integrate multiple impacts of agricultural systems, such as diets, health and greenhouse gas emissions. For example, studies have investigated the optimal average dietary intakes to minimise GHG emissions from agriculture (Willett *et al* 2019), or have quantified health benefits from dietary changes, alongside impacts on GHG emissions (Tilman and Clark 2014, Springmann *et al* 2016a, 2016b, 2017, 2018). Other studies, such as Clark *et al* (2019) have assessed a broader set of environmental impacts of agricultural systems (greenhouse gas emissions, eutrophication, land use, water resources), alongside the dietary health impacts. These studies have assessed changes in agricultural systems and their impacts on health and environmental impacts, in addition to GHG emissions. However, these earlier integrated agricultural models do not consider some key impacts, specifically, the health impacts associated with air pollutants from agricultural emissions, which have been shown to be effective in helping to raise climate change mitigation ambition (CCAC SNAP 2019).

Due to the benefits of designing integrated strategies that mitigate climate change and improve human health, and the lack of modelling tools to facilitate the assessment of these strategies, the aim of this paper is to describe an agricultural system model that for the first time integrates assessment of GHG emissions, and air pollution-associated health impacts, and the malnutrition (infant mortality associated with child stunting and low birth weight due to maternal malnutrition), high body-mass index (BMI), and dietary health impacts associated with food consumption. These health outcomes were included because they could be directly linked to widely available food consumption and production statistics. Other health outcomes associated with food consumption, such as those attributable to food-borne diseases (WHO 2015), could not be included in the model. The model is applied to quantify the global health impacts of agricultural production systems and impacts of agricultural production on climate change through emissions of GHGs and short-lived climate forcers between 2014 and 2018. The objective of this paper is to develop an integrated modelling framework for GHG emissions, air pollution and dietary, malnutrition and obesity health impacts from agriculture, and to validate the model by comparing against previous studies estimating these impacts separately and independently. However, it has the potential to evaluate future projections of food demand, and the human health and environmental consequences of that production, facilitating the development of integrated strategies to benefit human health, mitigate climate change and minimise the environmental impacts of agricultural systems. Demonstrating the consistency of results from the modelling framework with previous studies will provide the basis for its future application to assess how these variables could change for different socioeconomic development, and policy trajectories.

## 2. Methods

### 2.1. Modelling framework

The overall modelling framework for assessing food consumption and production is shown in figure 1. The model is designed for national scale application, and comprises four main modules that characterise different aspects of agricultural systems, and the emissions associated with them, as well as a health impact assessment module. Agricultural Demand (section 2.2) quantifies the domestic production of different crops, meat and dairy products based on the calorific intake of the average population, and the proportion of that intake that is met by different products. The Livestock (section 2.3) module characterises the livestock production systems, herd structure, feed and manure systems to meet demand for meat and dairy products. The Crop Production (section 2.4) and Pastureland (section 2.5) modules model the crop yield and pastureland productivity based on the demand for crops, silage and grass, and the nitrogen inputs to crop and pastureland based from manure,

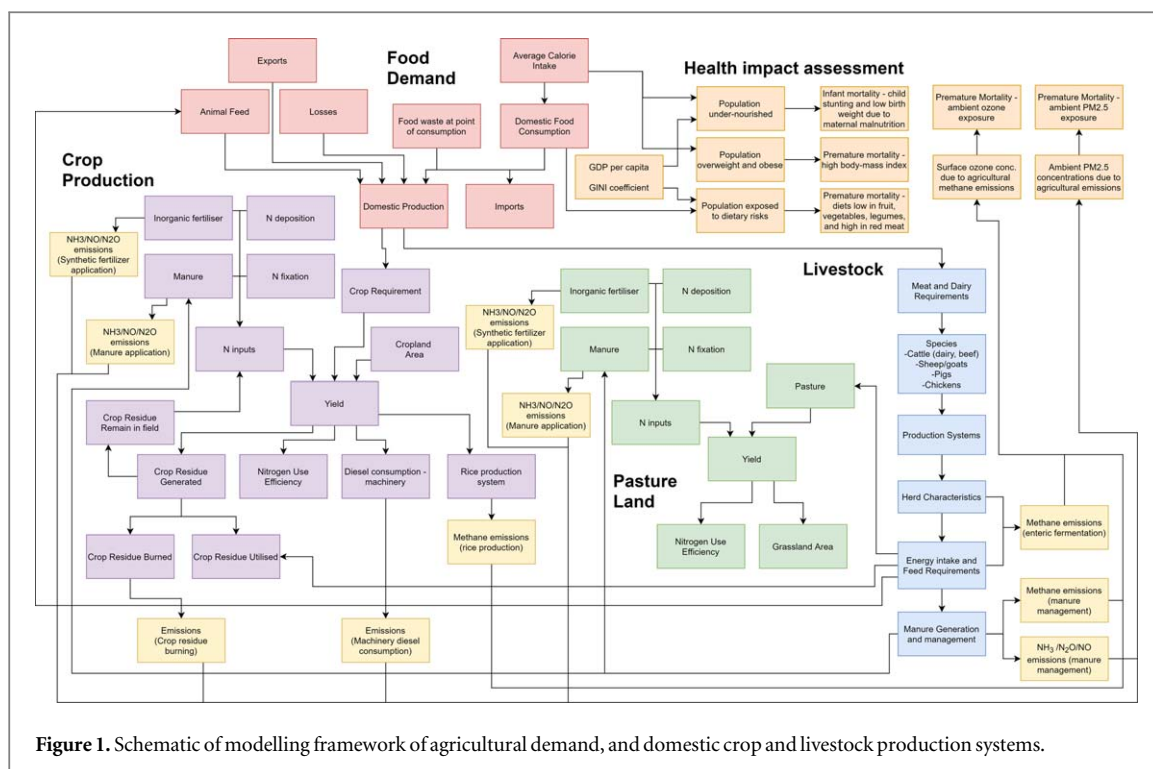


**Figure 1.** Schematic of modelling framework of agricultural demand, and domestic crop and livestock production systems.

synthetic fertilisers, deposition and nitrogen fixation. These modules also quantify the emissions associated with fuel consumption for agricultural machinery (section 2.6). The model is open-source, and the source code available at: <https://github.com/chmalle41/aghealth>.

Within the four modules characterising agricultural demand, and production, different impacts of the agricultural systems are characterised. These impacts specifically include (i) emissions of air pollutants and greenhouse gases, (ii) human health impacts associated with malnutrition for the proportion of the population estimated to be undernourished, (iii) human health impacts associated with diets low in fruits, vegetables, legumes, whole grains, fibre, nuts and seeds, and calcium, and high in red meat, and trans fatty acids, (iv) human health impacts associated with high body-mass index, and (v) human health impacts associated with air pollutants from agricultural emissions resulting from agricultural air pollution emissions. The methods associated with these human health impacts are described in section 2.7.

In this study, the model is used to characterise agricultural health and environmental impacts for historical years between 2014 and 2018. The years 2014–2018 were selected as the most recent years for which the majority of variables (described in the following sub-sections) required for the modelling were available, and to provide an indication of inter-annual variability in the GHG and air pollutant emissions and health impacts. The model has national-scale resolution, and, consistent with international emission inventory guidelines (IPCC 2006, EMEP/EEA 2019), emissions assigned to countries are those occurring within national boundaries. Similarly, the health impacts reported for each country are those health impacts occurring to the population of the country. The model includes impacts related to emissions and agricultural products produced in the country of interest and other countries via international trade and the transboundary movement of pollution. For example, for Country X, the health impacts quantified include those associated with food consumption (diet, malnutrition, and overweight/obesity) occurring to the population within Country X (and including health impacts associated with food consumed in Country X that was produced in Country X, and that was imported to Country X from Country Y). The health impacts in Country X also include those that result from the exposure of the population of Country X to air pollutants from agricultural emissions. This exposure, and attributable health burden, includes exposure resulting from agriculture emissions in Country X, as well as agricultural emissions in Country Y, the latter which leads to air pollution that is transported via the atmosphere to Country X. The data used in each of the modules for this application is described in the sub-sections below. The model can also be applied to assess future changes in agricultural health and environmental impacts through the creation of scenarios that project calorie intake and demand for agricultural products, and changes in the agricultural production systems over time.

## 2.2. Agricultural Demand

The agricultural demand module has been adapted from the modelling framework outlined in the Polestar model (Electris *et al* 2009). The starting point for modelling demand for different agricultural products (crops,

meat and dairy) is the average calorific intake of the population (calories per day). The product of average calorific intake and the population provides the total energy demand for food for the target country (equation 1). The proportion of these food (energy) requirements that are met from different crops, meat and dairy products is then used to calculate the total number of calories of these products that are required to meet the calorific demand (equation 2). The disaggregation of crop, meat and dairy products was based on the breakdown outlined in the FAOStat food balances (faostat.org), and is listed in table 1.

$$Cal_{tot} = Cal_{daily} \times Pop. \times 365 \quad (1)$$

Where  $Cal_{tot}$  (kCal  $y^{-1}$ ) is the total annual calorie intake for a given Population (Pop.) and  $Cal_{daily}$  (kCal  $person^{-1} day^{-1}$ ) is the per capita daily calorie consumption.

$$Cal_p = Cal_{tot} \times Frac_{cal} \quad (2)$$

Where  $Cal_p$  (kCal  $y^{-1}$ ) is the total annual calorie intake for a given Population (Pop.) that is consumed as product P and  $Frac_{cal}$  is the fraction of the average person's diet that is consumed as Product P.

In order for the total food requirements of a particular product to be translated into the domestic production of that product (to feed in to the livestock, crop and pasture modules described below), the total calories that are met by a product were converted into the tonnes required of the product based on the ratio of calories per tonne of product (equation 3). This domestic consumption of a particular food product was then converted into the domestic production, accounting for imports of the product, losses, and exports of the product (equation 4). For crops specifically, the tonnes of crop required for animal feed (in addition to human consumption) is added to the domestic production requirements, as an output from the livestock module (see section 2.3 for more details). The outputs from this module are the tonnes of crop, meat and dairy products required to meet the diet of the population of the target country.

$$Cons._p = Cal_{tot} \times R_p \quad (3)$$

Where  $Cons._p$  (tonnes  $y^{-1}$ ) is the total tonnes of Product P consumed in a country annually, and  $R_{prod}$  is the ratio of calories per tonne of Product P.

$$Prod_p = Cons._p + Ex._p + Loss._p + Feed._p - Im._p \quad (4)$$

Where  $Prod._p$  (tonnes  $y^{-1}$ ) is the domestic production of Product P, and  $Ex._p$  (tonnes  $y^{-1}$ ),  $Loss._p$  (tonnes  $y^{-1}$ ),  $Feed._p$  (tonnes  $y^{-1}$ ), and  $Im._p$  (tonnes  $y^{-1}$ ), are the annual exports, losses, feed requirements and imports of Product P, respectively.

For the years 2014–2018, the FAO food balances were used to obtain the inputs variables for the agricultural demand model, specifically per capita daily calorie consumption, and calories to tonne ratio, exports, imports, and losses for each agricultural product (<http://www.fao.org/faostat/en/#data/FBS>). Animal feed requirements for crops were obtained from the livestock module described in section 2.3 below.

### 2.3. Livestock production systems

The livestock module is adapted from the FAO Global Livestock Environmental Assessment Model (GLEAM) (FAO 2018). GLEAM is a model that is designed to quantify the greenhouse gas emissions from livestock production systems, and has been widely used for greenhouse gas mitigation assessments. However, GLEAM is designed only to assess the livestock system, including the herd structure, feed requirements and manure management for different species and livestock systems. Therefore, the modelling framework described in GLEAM was adapted and modified to be integrated with the agricultural demand module, and the crop and pastureland modules included here.

The livestock module includes four animal categories, cattle, sheep/goats, pigs and chickens. The primary input to the livestock module is the tonnes of meat, dairy and eggs that are required and output from the agricultural demand module. These inputs are then converted into the total number of animals in each herd based on the average carcass weight, and offtake rate for meat (equation 5), and the average milk production per head for dairy (equation 6).

$$Animals_s = \frac{Prod_p}{\frac{CW}{OR}} \quad (5)$$

where  $Animals_s$  is the total number of animals of species S in the herd, CW is the carcass weight (tonnes), and OR is the offtake rate (fraction of total herd culled per year).

**Table 1.** Breakdown of crop, meat and dairy products used to model demand and production taken from food energy balance.

Crops	Meat/Dairy			
Cereals	Barley and Products	Bovine meat (Cattle)		
	Maize and Products			
	Millet and Products			
	Oats			
	Rice			
	Rye and Products			
	Sorghum and Products			
	Wheat and Products			
	Other Cereals			
	Fruits		Apples and Products	Dairy (Cattle)
			Bananas	
Other Citrus				
Dates				
Other Fruits				
Grapefruits and Products				
Grapes				
Lemons, Limes and Products				
Oranges, Mandarines				
Pineapples and products				
Plantains				
Nuts	Nuts and Products	Mutton & Goat Meat (Sheep/goat)		
Oilcrops	Coconuts	Other dairy (Sheep/goat)		
	Groundnuts			
	Oilcrops, other			
	Olives			
	Rape and Mustard Seed			
	Sesame Seed			
	Soyabeans			
Pulses	Beans	Pigmeat (Pigs)		
	Peas			
	Pulses			
Roots	Cassava and Products	Poultry Meat (Chickens and other poultry birds)		
	Potatoes and Products			
	Other Roots			
	Sweet Potatoes			
	Yams			
Stimulants	Cocoa Beans and products	Eggs (Chickens and other poultry birds)		
	Coffee and Products			
	Tea			
Sugar	Sugar cane			
	Sugar beet			
Vegetables	Onions			
	Tomatoes and Products			
	Other vegetables			
Vegoils	Palm Oil			
	Palmkernel Oil			
	Rape and Mustard Oil			
	Sesameseed Oil			
	Soyabean Oil			
	Sunflowerseed Oil			

$$Animals_{d,s} = \frac{\frac{Prod_d}{Frac_{d,s}}}{MP_s} \quad (6)$$

**Table 2.** Breakdown of livestock management categories and cohorts that livestock are disaggregated into.

Parameter	Cattle	Sheep/goats	Pigs	Chickens
Livestock Management systems	Mixed	Mixed	Backyard	Backyard
	Grassland	Grassland	Intermediate	Layers
	Feedlot	Feedlot	Industrial	Broilers
Animals	Dairy Beef	Dairy Beef		
Cohort	Adult Females	Adult Females	Adult Females	Adult Females
	Adult Males	Adult Males	Adult Males	Adult Males
	Replacement Females	Replacement Females	Replacement Females	Replacement Females
	Replacement Males	Replacement Males	Replacement Males	Replacement Males
	Meat Females	Meat Females	Meat Animals	Adult laying females (layers)
	Meat Males	Meat Males		Surplus males (backyard)
	Feedlot Meat Females			Surplus females (backyard, layers)
	Feedlot Meat Males			Meat animals (broilers)

Where  $\text{Animals}_{d,s}$  is the number of dairy live animals for species  $S$  in the herd,  $\text{Prod}_d$  is the total annual domestic milk production,  $\text{Frac}_{d,s}$  is the fraction of total milk production produced by species  $S$ , and  $\text{MP}_s$  is the annual per head milk production for species  $S$ .

### 2.3.1. Herd structure

The number of live animals is then combined with other input variables to characterise the structure of the herd for cattle, sheep/goats, pigs and chickens. The disaggregation of the herd into different management systems, and cohorts is specified in table 2, and follows the GLEAM modelling framework. Additional inputs include the fraction of livestock that are managed in different livestock management systems, male to female ratios, the mass of animals at different life stages, and death, fertility and replacement rates for each species in the target country. The fraction of livestock managed from different livestock production systems for each country was calculated by combining the gridded Global Livestock Production System database which characterises the type of livestock production system in 0.083 degree grids globally, with gridded global livestock numbers, to estimate the total number of animals being managed in different livestock systems (Robinson *et al* 2011). All other input parameters were regional defaults specified in the GLEAM modelling documentation (FAO 2018). The outputs from the herd module are the number of animals in a given year in each cohort for each livestock management system shown in table 2. Additional outputs include live weights and daily weight gains for replacement animals.

### 2.3.2. Energy intake and feed

The herd module then feeds into the characterisation of the energy intake and feed requirements of a given animal herd. The energy intake is calculated separately by cohort, and livestock management system for each species, following the methodology outlined in GLEAM (FAO 2018). Energy requirements are calculated based on the net energy required for maintenance (dependent on live weight of animal of particular cohort), activity (dependent on time spent grazing versus in housing), growth (for replacement and fattening animals), milk production (for adult female dairy cattle and sheep/goats), pregnancy, and fibre production (sheep/goats). The total energy required for a particular animal cohort is then converted into the dry matter intake (DMI, kg dry matter head<sup>-1</sup> day<sup>-1</sup>) based on the digestibility of the feed that the animal cohort is fed.

The composition of the animal feed is the percentage of DMI that is provided as roughages, cereals, by products, concentrates, or swill (pigs only). In GLEAM, 29 and 42 categories of feed materials are specified for cattle/sheep/goats and pigs/chickens, respectively, and the composition of the animal feed is determined based on crop yield and pasture productivity data. In this study, the model retains the same feed categories. However, the aim of this model is to explore crop yield and pasture productivity based on demand for crops and grasses (for human and animal feed). Therefore, the composition of the feed is directly entered in the livestock model as the percentage of the feed composition that is met by a particular feed product, so the outputs (tonnes of feed required for each category) can feed in to the crop and pasture modules (sections 2.4 and 2.5).

The composition of the feed for a particular cohort in a particular management system is used first to calculate the average digestibility (%), and gross energy (GE) content of the overall feed (MJ kg DM<sup>-1</sup>), based on the individual digestibility and gross energy contents of the individual feed components. These variables are then used to calculate the DMI of animals in a particular cohort and management system, as described in GLEAM (FAO 2018). Once the DMI has been determined, the total dry matter feed requirements for each feed group was calculated as the product of the DMI, number of animals in a cohort and management system, and the fraction

of the overall feed that comes from a particular feed group. For the feed groups that are particular crops/feed crops, or roughages (grass, legumes etc), the total dry matter required was used as an input to the agricultural demand, and pastureland modules, respectively (described in sections 2.2 and 2.5). For the feed groups that are crop residues, the total crop residue requirements were used as input to determine the use of crop residue produced in the crop production module, and is subtracted from the total residue generated to give the remaining residue to be allocated between being used for other productive purposes, reintegrated into the soil, or burned (see section 2.4 for more details).

The DMI was further used to quantify methane emissions from enteric fermentation for cattle, sheep/goats and pigs based on the IPCC Tier 2 approach outlined in IPCC (2006), and shown in equation 7.

$$CH_{4EF, s, c, m} = N_{s, c, m} \times 365 \times GE_{s, c, m} \times DMI_{s, c, m} \times \frac{Y_{m, s, c, m}}{55.65} \quad (7)$$

Where  $CH_{4, EF, s, c, m}$  is the methane emissions from enteric fermentation for species S, cohort C, in management system M,  $N_{s, c, m}$  is the number of animals of species S, cohort C, in management system M, and  $Y_{m, s, c, m}$  is the percentage of energy in feed converted to methane (calculated from the digestibility of the feed for cattle and sheep/goats).

### 2.3.3. Manure production and management

The DMI is then used to determine the mass of manure generated by each animal species, cohort and management system. In the manure module, first, methane emissions are estimated based on the volatile solids (VS, kg head<sup>-1</sup> day<sup>-1</sup>) excreted by each animal in a particular cohort and management system, which is determined by the DMI and digestibility of the animal feed. The methane emissions are the estimated using equation 8, based on Tier 2 methods in IPCC (2006).

$$CH_{4Man, s, c, m} = N_{s, c, m} \times 365 \times VS_{s, c, m} \times B_o \times 0.67 \times \sum^{mms} (mcf \times Frac_{mms, s, c, m}) \quad (8)$$

where  $CH_{4, Man, s, c, m}$  is the methane emissions from manure management for species S, cohort C, in management system M,  $B_o$  (m<sup>3</sup> CH<sub>4</sub> kg VS<sup>-1</sup>) is the maximum methane producing capacity for species S, cohort C, in management system,  $mcf$  is the methane correction factor (fraction) for each manure management system, and  $Frac_{mms}$  is the fraction of manure handled within each manure management system for species S, cohort C, in management system M. The manure management systems are disaggregated based on the manure management systems included in GLEAM (FAO 2018), and include pasture/grazing, daily spread, solid storage, dry lot, liquid slurry, anaerobic lagoon, anaerobic digester, pit storage, composting, burned for fuel, and poultry manure with litter. The methane correction factors for each manure management system were estimated based on the methodology outlined in GLEAM (FAO 2018).

The manure module was also used to estimate the nitrogen excreted from animals in each cohort and management system, to be used as an input to the crop production and pastureland modules described below, and to estimate the emissions of nitrous oxide (N<sub>2</sub>O), ammonia (NH<sub>3</sub>) and nitrogen oxide (NO). The nitrogen excreted by animals in each cohort and management system was calculated using the methodology outlined in GLEAM (FAO 2018). First, the nitrogen content of the DMI is calculated based on the nitrogen content of each feed group, and the contribution of that feed group to the overall DMI. The nitrogen excreted is then calculated based on the total nitrogen content of the dry matter intake, subtracting the nitrogen that is retained by an animal in each cohort and management system. The nitrogen retention varies by animal and cohort, and is a function of milk/egg production, weight gain, and reproduction, and is calculated as outlined in GLEAM (FAO 2018), and IPCC (2006).

The GLEAM model only estimates methane and N<sub>2</sub>O emissions from manure management, and does not quantify air pollutant emissions (NH<sub>3</sub>, NO), or the manure nitrogen available for application to crop and pasturelands as fertiliser. To account for these additional aspects of the nitrogen flows within the livestock manure systems, an alternative methodology based on EMEP/EEA (2019) emission inventory guidebook Tier 2 method was used instead. The total nitrogen excreted for each animal, by cohort and management is used as input to model the fate of the nitrogen excreted. The model tracks the nitrogen that is excreted and what fraction is emitted to the atmosphere as N<sub>2</sub>O, NH<sub>3</sub> and NO, what fraction is leached from the system as nitrate (NO<sub>3</sub>), and what fraction is available for application on fields, and used as inputs to the crop production and pastureland models described below. The nitrogen is tracked as total nitrogen, and as total ammoniacal nitrogen (TAN) which is used to calculate ammonia emissions from manure management (by default, the fraction of total N which is TAN is set to 0.6 (EMEP/EEA 2019)). The output from this module used as input to the crop and pastureland modules described below is the nitrogen available for application to fields (N<sub>applic</sub>, tonnes N y<sup>-1</sup>), which is calculated as shown in equation 9.

$$N_{applic} = N_{direct} + N_{stored} - N_{NH_3\ storage} - N_{NO\ storage} - N_{N_2\ storage} - N_{N_2O\ direct} - N_{leach} \quad (9)$$

Where  $N_{direct}$  is the nitrogen directly applied to fields (i.e. not stored),  $N_{stored}$  is nitrogen stored,  $N_{NH_3\ storage}$ ,  $N_{NO\ storage}$ ,  $N_{N_2\ storage}$ , and  $N_{N_2O\ storage}$  are the  $NH_3$ , NO,  $N_2$  and direct  $N_2O$  emissions from storage of manure, and  $N_{leach}$  is the mass of nitrogen leached. Equation 9 is applied separately for solid and slurry manure management systems, and is applied to total nitrogen, and to TAN separately. In addition to the  $NH_3$ , NO,  $N_2$  and direct  $N_2O$  emissions from solid and slurry storage of manure included in equation 9, the manure module also quantifies  $NH_3$  emissions from handling of manure excreted in yards and housing, and indirect  $N_2O$  emissions associated with (i) the  $NH_3$  and NO emissions from manure, and (ii) nitrogen leached from the manure management systems.

As outlined in EMEP/EEA (2019), first, the nitrogen excreted in housing, open yards, and while grazing is calculated, based on user-defined percentages of time that animals in a particular cohort and system spend in housing, yards and on pasture. For the nitrogen excreted during housing, this is split into the nitrogen (and TAN) handled as slurry, and as solid, based on the same manure management system fractions used in equation 8 above). Ammonia emissions from nitrogen excreted on yards and housing (slurry and solid) are then estimated by multiplying the TAN by ammonia specific emission factors, as outlined in EMEP/EEA (2019). For manure excreted in housing that is handled as solid, the N included in bedding is added to the N excreted by animals, according to EMEP/EEA (2019) methodologies that estimates the N added from straw bedding, based on the number of animals, the proportion of time spent in housing, and the N content of bedding.

The N (and TAN) that is handled as slurry and solid is then separated based on the proportion of the manure that is stored before application to fields (which gives  $N_{stored}$  in equation 9), used to produce biogas, applied directly onto fields without storage ( $N_{direct}$  in equation 9), and burned for fuel (solid only). The fraction of manure apportioned to each of these uses is input by the user. Emissions of  $NH_3$ , NO and  $N_2$  ( $N_{NH_3\ storage}$ ,  $N_{NO\ storage}$ ,  $N_{N_2\ storage}$ ) from solid and slurry storage are then calculated by multiplying the TAN stored as slurry/solid by management specific emission factors (EMEP/EEA 2019). Direct  $N_2O$  emissions ( $N_{N_2O\ direct}$ ) are calculated by multiplying the total N stored using different manure management systems (those defined for methane manure emissions above) and management specific emission factors.

Finally, indirect  $N_2O$  emissions from volatilisation were calculated by multiplying the N emitted as  $NH_3$  and NO from manure storage by an  $N_2O$  specific emission factor. Indirect  $N_2O$  emissions from N leached from each manure management system were calculated by multiplying the N stored under each manure management system by the fraction of N leached from each system, and a  $N_2O$ -specific emission factor.

## 2.4. Crop production

The crop production module takes as input the domestic production of different crops ( $Prod_{crop}$ , shown in table 1) from the agricultural demand module, and estimates the crop yield ( $Y_{crop}$ , tonnes  $ha^{-1}$ ) required to produce the domestic quantity of crop demanded, based on the area harvested for each crop obtained from the FAOSTAT database (equation 10). The crop production module includes crops for direct human consumption, as well as feed crops used for animal feed (figure 1).

$$Y_{crop} = \frac{Prod_{crop}}{Land_{crop}} \quad (10)$$

In addition to the yield, the outputs from this module include the nitrogen use efficiency (NUE, the fraction of the nitrogen input into the system that is taken up and used by the plant), and the crop residue that is generated. To model NUE, five sources of nitrogen inputs are combined to estimate the total nitrogen inputs ( $N_{inputs}$ ,  $kg\ N\ ha^{-1}\ y^{-1}$ ), i) biological nitrogen fixation, ii) nitrogen deposition, iii) manure nitrogen, iv) inorganic nitrogen fertiliser, and v) crop residues from the previous harvest that remain in the field and which are incorporated back into the soil (equation 11).

$$N_{inputs} = N_{fix} + N_{dep} + N_{manure} + N_{inorg} + N_{cr} \quad (11)$$

The inputs of nitrogen from biological fixation ( $N_{fix}$ ) was set to  $5\ kg\ N\ ha^{-1}\ y^{-1}$  for all crops except rice, where  $25\ kg\ N\ ha^{-1}\ y^{-1}$  was used, based on values assigned in Lassaletta *et al* (2016). Nitrogen deposition inputs ( $N_{dep}$ ) values were estimated by calculating national crop production-weighted total nitrogen deposition using  $2 \times 2.5^\circ$  global gridded total nitrogen deposition from Geddes *et al* (2017), which was available for the years 2014–2016, and gridded crop production maps from the Spatial Production Allocation Model (SPAM, (International Food Policy Research Institute 2019, 2020)). Inputs of nitrogen from manure ( $N_{manure}$ ) were based on the nitrogen available for application estimated using equation 9. The total manure N (and TAN) available for application (disaggregated by solid and slurry) was split between the proportion applied to crop lands, and proportion applied to grasslands (by default 90% was assumed to be applied to crop lands, based on Lassaletta *et al* 2016), and divided by the total crop land in the target country to estimate the  $kg\ N$  applied per

hectare per year (assuming the same application rate of manure across all crops). The application rate of inorganic fertiliser was also calculated by splitting the total inorganic fertiliser applied in each country (obtained from FAOStat) between crop lands and pasturelands as described in Lassaletta *et al* (2014). The total inorganic fertiliser nitrogen applied to crop lands was then divided by the total cropland area to give the synthetic fertiliser application rate ( $\text{kg N ha}^{-1} \text{y}^{-1}$ , again assuming the same application rate for all crops). Finally, the N applied from the incorporation of crop residues back into the soil was based on the N contained within the crop residues produced during the previous years, subtracting the crop residues that were removed for feed or fuel, or burned (see below for description of methods for estimating crop residue use).

$Y_{crop}$  was converted to the crop yield in terms of nitrogen contained in the crop ( $Y_{Ncrop}$ ,  $\text{kg N ha}^{-1} \text{y}^{-1}$ ), based on the proportion of nitrogen contained in each crop ( $N_{crop}$ ) using equations 12, and 13 was used to estimate NUE.

$$Y_{Ncrop} = \frac{Y_{crop}}{N_{crop}} \quad (12)$$

$$NUE_{crop} = \frac{Y_{Ncrop}}{N_{inputs}} \quad (13)$$

For the model to be able to assess how crop yields could change in response to changes in overall N inputs, the theoretical maximum yield ( $y_{max}$ ,  $\text{kg N ha}^{-1} \text{y}^{-1}$ ) is also calculated using the methodology outlined in Lassaletta *et al* (2016, 2014), and shown in equation 14. For future model applications that assess future scenarios with changing nitrogen inputs equation 14 is rearranged to estimate future crop yields based on a given  $y_{max}$  and nitrogen input.

$$y_{max} = \frac{Y_{Ncrop} * N_{inputs}}{N_{inputs} - Y_{Ncrop}} \quad (14)$$

The application of manure nitrogen is associated with emissions of  $\text{NH}_3$ , NO and  $\text{N}_2\text{O}$ , which are estimated based on EMEP/EEA (2019) and IPCC (2006) methodologies. For each pollutant, the tonnes of N (for direct  $\text{N}_2\text{O}$  and NO) and TAN (for  $\text{NH}_3$ ) applied as solid and slurry are multiplied by pollutant and management-specific emission factors (EMEP/EEA (2019) (Tier 2 emission factors by default for NO and  $\text{NH}_3$ , IPCC 2006 Tier 1 default emission factors for  $\text{N}_2\text{O}$ ). Indirect  $\text{N}_2\text{O}$  emissions associated with emissions of  $\text{NH}_3$  and NO, and through leaching were also calculated using the same methods as described in section 2.3 for manure storage. Similarly, for inorganic fertilisers, fertiliser-specific emission factors for  $\text{NH}_3$ , NO and direct  $\text{N}_2\text{O}$  emissions were combined with the tonnes N applied for each inorganic fertiliser to estimate the quantity of emissions. Indirect  $\text{N}_2\text{O}$  emissions were estimated using the same approach as for manure application.

For each crop, the tonnes of crop residues produced from its production was calculated using the IPCC (2006) Tier 2 methodology. The tonnes of crop dry matter produced are first multiplied by a crop-specific factor that converts tonnes crop production to tonnes of above-ground residue biomass. Crop-specific ratios of above-to-below ground biomass were used to estimate the tonnes below-ground residue biomass produced. The tonnes of crop residue produced were then apportioned between different categories, (i) removal for fuel, (ii) removal for feed, (iii) openly burned in field, and (iv) remains in field. The tonnes of crop residue removed for fuel is determined by a user-defined proportion of above-ground residue used for fuel. The tonnes of crop residue used for feed is obtained directly from the livestock module, as described in section 2.3. The proportion of the remaining residue (i.e. not removed) which is burned is a user-defined parameter, and was set to 25% of crop residue remaining in the field for regions in Latin America, Africa and Asia, and 0% for Europe and North America, based on IPCC (2006) and consistent with Yevich *et al* (2003). Any residue not burned is assumed to be incorporated back into the soil, and constitutes the  $N_{cr}$  variable in equation 11. For the tonnes of residue estimated to be burned, emissions of air pollutants (carbon monoxide, nitrogen oxides, sulphur dioxide, volatile organic compounds, ammonia,  $\text{PM}_{10}$ ,  $\text{PM}_{2.5}$ , black carbon, organic carbon, and methane) are estimated using default emission factors outlined in EMEP/EEA (2019).

Methane emissions from rice production were calculated using the IPCC (2019b) Tier 1 methodology, shown in equation 15, accounting for different water regimes used to produce rice in the target country.

$$Emis_{CH_4} = \sum (EF_w * t_w * A_w) \quad (15)$$

Where  $EF_w$  is the daily methane emission factor for rice production,  $t$  is the cultivation period (days), and  $A$  is the area under cultivation using a particular water management regime  $w$ . The emission factor for each water management regime is calculated by scaling a baseline emission factor by a series of factor representing the type of water regime before and during the cultivation period, as well as accounting for any organic amendments, as shown in equation 16.

$$EF_w = EF_c * SF_w * SF_p * SF_o \quad (16)$$

Where  $EF_c$  is the baseline emission factor for continuously flooded fields,  $SF_w$  is the scaling factor for different water management regimes during the cultivation period,  $SF_p$  is the scaling factor for the water management regime before the cultivation period, and  $SF_o$  is the scaling factor for the organic amendments applied. For  $EF_c$ , default regional values from IPCC (2019b) were used, and the default scaling factors for different water regimes from IPCC (2019b) were also used. For  $t$ , the rice growing seasons described in Laborte *et al* (2017) for different rice growing areas globally were used. For each country, the average cultivation period was calculated as an area-weighted average of all data points for that country included in Laborte *et al* (2017). In addition, an area-weighted average number of growing seasons was calculated for each country from the Laborte *et al* (2017) rice growing calendars, and multiplied by the land area used for rice production to reflect the total area cultivated across the year. For those countries not covered in Laborte *et al* (2017), IPCC (2019b) regional default values of  $t$  were used. The total land area was divided between different water regimes to estimate  $A_w$ . Due to limitations in the availability of global information on the water regimes used for rice production, the total land area used for rice production was disaggregated into two water regimes, (i) irrigated, and (ii) rainfed and deep water. The Spatial Production Allocation Model (SPAM) provides globally gridded data on the land area used for the production of different types of crops (Yu *et al* 2020). For each country, the total land area used for rice production categorised as irrigated and as rainfed in the SPAM dataset were summed and used to calculate the percentage of irrigated and rainfed land used for rice production in each country. This percentage is then applied to  $Land_{rice}$  from equation 10 to estimate the  $A_w$  for irrigated and rainfed crops.

## 2.5. Pasturelands

The productivity of pasturelands was calculated using a similar approach as outlined above for crop production. First, N inputs to grasslands were estimated using equation 11 (with  $N_{cr}$  set to zero). Biologically fixed N was set to  $5 \text{ kg N ha}^{-1} \text{ y}^{-1}$ , and N deposition was obtained from the same gridded N deposition dataset as for crop production. As outlined in section 2.4, for both manure N applied, and inorganic N applied, the total N available for application from manure and inorganic fertiliser are split based on the user-defined proportion of manure and inorganic fertiliser applied to crop land and pastures. For the proportion of manure N and inorganic fertiliser applied to pastureland, these totals were divided by the total pastureland for each country (obtained from FAOStat). For pasturelands, an additional N input is the manure N applied by animals during grazing. This is added to the manure N applied to pastureland from storage, and divided by the total pastureland to obtain the overall  $\text{kg N ha}^{-1} \text{ y}^{-1}$  from manure applied to pasturelands.

Emissions from the application of manure (applied after storage, and through grazing) were estimated using the same approach as described in section 2.4. The total N (or TAN for  $\text{NH}_3$ ) applied to pasturelands was multiplied by pollutant ( $\text{NH}_3$ , NO, direct  $\text{N}_2\text{O}$ ) and management (slurry, solid and grazing)-specific emission factors, from EMEP/EEA (2019) and IPCC (2006). For inorganic fertiliser application, the same approach as for croplands was applied to estimate  $\text{NH}_3$ , NO, direct and indirect  $\text{N}_2\text{O}$  emissions from inorganic fertiliser application to pastures.

The NUE for pastures was then estimated using equation 15, where  $N_{inputs}$  are the tonnes N input, estimated as described above, and  $N_{outputs}$  are the tonnes N that are produced from the pastureland.

$$NUE_{pasture} = \frac{N_{outputs}}{N_{inputs}} \quad (17)$$

$N_{outputs}$  are estimated based on the requirements for grass and other roughages from pastureland from the livestock module described in section 2.3. The tonnes of grass and other roughages required as feed in the livestock model is multiplied by the nitrogen content to estimate  $N_{outputs}$ .

## 2.6. On-farm energy consumption

In addition to the emissions described above, on-farm 'direct' energy consumption associated with livestock and crop production is also associated with emissions of greenhouse gases and air pollutants. Sources of energy consumption on farm include the use of machinery (tractors, harvesters, threshers etc), mechanical pumps for irrigation, as well as infrastructure development, drying crops, heating and lighting, transport etc In this study, the emissions associated with fuel (diesel) consumption associated with farm machinery was estimated according to equation 18, where  $FC_{mach}$  is the total diesel consumption for machinery (GJ),  $LA_{crop}$  is the land area for crop production derived in equation 13, and  $FH$  is the per hectare fuel consumption for machinery.

$$FC_{mach} = LA_{crop} * FH \quad (18)$$

$FH$  was derived for each country by first summing the number of agricultural tractors, and harvesters/threshers included in the FAOStat database for the most recent year available. This number was then multiplied by regional per unit fuel consumption values for agricultural machinery used in Pellegrini and Fernández (2018). The total fuel consumption for agricultural machinery for the most recent year in the FAOStat database was then divided by the total crop area in that year (also from FAOStat), and used in equation 18 to estimate the total fuel

consumption from agricultural machinery that is consistent with the crop production model described in section 2.4. The total diesel consumed was then multiplied by IPCC (2006), and EMEP/EEA (2019) Tier 1 emission factors for diesel combustion to estimate greenhouse gas and air pollutant emissions from agricultural machinery, respectively. Other direct, on-farm emissions associated with energy consumption were not quantified, such as mechanised irrigation, electricity consumption for heating and lighting, due to lack of data globally on the energy mixes for different on-farm activities. Arizpe *et al* (2011) estimated that for the majority of countries evaluated, machinery fuel consumption was the largest sources of direct on-farm energy consumption (21 countries were evaluated).

In addition, agricultural activities also demand substantial indirect off-farm energy consumption, that exceed the on-farm consumption, e.g. for fertiliser production and the processing and distribution of products (Arizpe *et al* 2011, FAO 2011, Pellegrini and Fernández 2018). There are substantial sources of emissions associated with these processes, but are outside the scope of this current work.

## 2.7. Health impact assessment

Characterising the demand for food, the agricultural system which produces this food, and the emissions of air pollutants and greenhouse gases that are produced from the livestock, crop and pasturelands in the agricultural system allows the different impacts that result from both food consumption and impacts from the particular agricultural systems producing it to be quantified. The impacts of food consumption that are quantified using this modelling framework include the health impacts from particular levels of calorific intake (i.e. malnutrition and high body-mass index), described in section 2.7.1, and from particular levels of intake of different types of foods (section 2.7.2). For the agricultural systems producing this food, the impacts quantified include the health impacts attributable to ambient air pollution exposure resulting from agricultural emissions (section 2.7.3).

For the health impacts from all risk factors (malnutrition, high BMI, dietary risks, and air pollution), the health endpoint quantified in the model is the number of premature deaths associated with a particular level of exposure to that risk. The number of premature deaths was calculated by age ( $a$ ), sex ( $s$ ), and disease ( $d$ ) using equation 19.

$$\Delta Mort = \sum_{a,s,d} \left( y_{o,a,s,d} * \frac{RR - 1}{RR} * pop_{a,s} \right) \quad (19)$$

Where  $\Delta Mort$  is the change in the number of premature deaths,  $y_o$  is the baseline mortality rate for disease  $d$ , for sex  $s$ , and age group  $a$ ,  $pop$  is the population of sex  $s$ , and age group  $a$  exposed to a given level of the risk factor, and  $RR$  is the relative risk associated with a particular level of exposure to a risk factor above the minimum risk exposure level. The population of each sex and age groups were taken from the UN Population Division 2019 revision (United Nations Department of Economic and Social Affairs Population Division, 2019), and the baseline mortality rates for each disease for each sex and age group were taken from the Global Burden of Disease 2019 study (Abafati *et al* 2020). The subsections below detail the specific diseases, relative risks, and assessment of exposure to each of the risk factors considered in the health impact assessment.

### 2.7.1. Health impacts from malnutrition and high body-mass index

The health impacts associated with malnutrition were infant mortality associated with child stunting, and infant mortality associated with the proportion of low birth weight births that were estimated to be due to intrauterine growth restriction (IUGR) associated with maternal malnutrition. The average calorie intake was converted into the proportion of the population undernourished using the method outlined in FAO (2003). Using this method, a frequency distribution of daily calorific intakes is developed based on the population average daily calorific intake (in FAO (2003) this is defined as the food availability, i.e. food available for consumption, including food waste), and a coefficient of variation which accounts for variation in household income, and variation in energy requirements. The component of the coefficient of variation due to household income is calculated as a function of per capita GDP and Gini coefficient (to represent income inequality), both of which were obtained from World Bank statistics. The component of the coefficient of variation due to energy requirements was fixed at 0.2, as outlined in FAO (2003). The frequency distribution constructed from the average daily calorie intake and coefficient of variation was assumed to be lognormal.

The proportion of the population undernourished is the proportion of the population consuming fewer than a minimum daily calorific intake. To account for the variation in demographics across countries, the minimum daily energy requirement was taken from FAO Food Security Indicators (<http://www.fao.org/economic/ess/ess-fs/ess-fadata/en/#.YCAr1mj7SUK>) for each country, and, where specific country data was not available, a regional average was calculated and used.

The proportion of the mothers malnourished in each country was assumed to be the same as the overall proportion of the population malnourished. The methodology outlined in Blössner *et al* (2005) was then used to quantify the number of pregnancies that experienced intrauterine growth restriction (IUGR) due to maternal

malnutrition (using a relative risk of 1.8 (1.7–2.0)). This value was then applied to overall number of IUGR-attributable low birth weight births in the country to estimate the number of low birth weight births attributable to maternal malnutrition. Finally, the number of neonatal deaths attributable to maternal malnutrition was estimated applying equation 19 in which  $pop$  was the number of IUGR-attributable low birth weights due to maternal malnutrition,  $y_o$  was the overall neonatal mortality rate, and RR was 6, representing the increased risk of death of IUGR low birth weight births compared to a normal weight birth.

For child stunting, the proportion of children (< 5 years old) suffering from moderate (>2 standard deviations below mean height-for-age) and severe (> 3 standard deviations) stunting was estimated from the average proportion of the population malnourished based on a model developed by Lloyd *et al* (2011). This model incorporates the proportion of the population malnourished, as well as ‘non-food causes’ of malnutrition, which is derived from per capita GDP and the Gini coefficient for each country. Child mortality associated with moderate and severe child stunting was estimated using equation 19, in which  $pop$  is the proportion of the population in each country under 5 that are moderately or severely stunted,  $y_o$  is the all-cause mortality rate for children under 5 (disaggregated between male and female), and RR is the increased risk of death for moderately (2.28 (1.91–2.72)) and severely (5.48 (4.62–6.50)) stunted children compared to children with average height-for-age, taken from Olofin *et al* (2013). In addition to child stunting, other metrics/risks, such as child wasting and child underweight have been applied to estimate health impacts from child malnutrition (Murray *et al* 2020), and have been shown to have a greater association with child malnutrition-attributable mortality. Child stunting was the metric used to quantify child malnutrition health impacts here due to the availability of a quantitative relationship between the overall proportion of the population malnourished, and child stunting (see section 3 for a description of the results in comparison to previous child malnutrition health impacts).

The relationship between the average daily calorie intake and the proportion of the population overweight (BMI > 25 kg m<sup>-2</sup>) and obese (BMI > 30 kg m<sup>-2</sup>) developed in Springmann *et al* (2016a) was used to calculate the number of people in each adult (>25 years) age category in each country that were overweight and obese for a given average daily calorie intake. The relationship developed by Springmann *et al* (2016a) was based on a linear regression of historical national data (1980–2009) on calorie intake and mean BMI globally. The number of premature deaths associated with high body-mass index were then calculated using the methods outlined in Murray *et al* (2020). Equation 19 was applied with  $y_o$  and RR the baseline mortality rates, and the relative risks compared to a BMI of 22.5 kg m<sup>-2</sup>, respectively, for the 37 diseases associated with high body-mass index in Murray *et al* (2020).

### 2.7.2. Health impacts from dietary risks

The number of premature deaths associated with different dietary risk factors were estimated for the proportion of the population whose average daily intake was below minimum risk exposure levels outlined in GBD 2017 Diet Collaborators (2019) for fruit (250 g day<sup>-1</sup>), vegetables (360 g day<sup>-1</sup>), legumes (60 g day<sup>-1</sup>), and milk (435 g day<sup>-1</sup>), and above the minimum risk exposure level for red meat (23 g day<sup>-1</sup>).

The average daily consumption of fruit, vegetables, legumes, milk and red meat was obtained from equation 3. The distribution of daily consumption of each food type across the population in each country was then estimated by first developing a distribution of per capita GDP, based on the Gini coefficient of each country. The frequency distribution of GDP per capita was assumed to be lognormally distributed. The average daily consumption of each food type was assumed to correspond to the average GDP per capita. At higher and lower levels of per capita GDP, the average daily consumption of each food type was assumed to vary with the change in per capita GDP, with an elasticity. Muhammad *et al* (2017) derived elasticities for different food types for different regions, based on an analysis across 164 countries. Regional elasticities for each food type were applied to construct the frequency distribution of daily consumption, to then derive the proportion of the population whose consumption of each food type was within a certain range.

To characterise both the proportion of the population consuming different food types below (fruit, vegetables, legumes, milk) or above (red meat) the minimum risk exposure level, and the degree of under or over consumption, for fruits, vegetables, legumes, , and milk, the range between the minimum exposure risk level, and 0 g day<sup>-1</sup>, was subdivided into 10 sub-groups (e.g. for fruits, 10 groups with consumptions between 250–225 g day<sup>-1</sup>, 225–200 g day<sup>-1</sup>, 200–175 g day<sup>-1</sup> ... 50–25 g day<sup>-1</sup> and 25–0 g day<sup>-1</sup>). The proportion of the population with daily average consumption within the range of each sub-group were then calculated. For red meat consumption, a set of X groups with consumption above the minimum risk level were set up to characterise the proportion of the population consuming different levels of red meat above the minimum risk level.

The disease categories associated with each dietary risk, and the relative risks (with the exception of red meat) for each disease, sex, and age category were taken from GBD 2017 Diet Collaborators (2019). This data was then used by applying equation 19 to estimate the number of premature deaths separately for each of the subgroups, in combination with the population in each of the subgroups. For red meat consumption, the Global Burden of

Disease disaggregates the health risks from red meat between two risk factors, i) unprocessed red meat, and ii) processed meat (which also includes processed white meat). The output from the agricultural model shown in figure 1 is the total red meat consumption, and therefore alternative relative risks developed total red meat consumption (unprocessed and processed) were identified for compatibility with the data on dietary intakes available from the model. Yip *et al* (2018) evaluated available meta-analyses to collate 'best identified' dose-response relationships between total red meat consumption and different health end points. The relative risks identified in Yip *et al* (2018) for cardiovascular diseases and cancer were applied to quantify the impact of total red meat consumption on premature mortality.

### 2.7.3. Ambient air pollution health risks

The health impacts (Premature mortality) attributable to exposure to ambient air pollution resulting from agricultural emissions were estimated for exposure to fine particulate matter (PM<sub>2.5</sub>) and ground-level ozone (O<sub>3</sub>). Emissions of primary PM<sub>2.5</sub> (black carbon and organic carbon), as well as PM<sub>2.5</sub>-precursors (NO<sub>x</sub>, SO<sub>2</sub>, NH<sub>3</sub>) from the agriculture sector were converted into population-weighted annual average PM<sub>2.5</sub> concentrations by i) gridding national total emissions across the country, and ii) combining emissions with coefficients from the GEOS-Chem adjoint model that quantify the sensitivity of changes in emissions of PM<sub>2.5</sub> and PM<sub>2.5</sub>-precursor pollutants in 2 × 2.5° grids globally to national population-weighted PM<sub>2.5</sub>. For livestock emissions, i.e. NH<sub>3</sub> and NO<sub>x</sub> emissions from manure management, emissions were gridded separately for each animal type and management system into 0.083° grids based on the FAO global gridded livestock of the world (GLW3) dataset (Gilbert *et al* 2018). Emissions associated with crop production were gridded into 0.083° grids based on the Spatial Production Allocation Model (SPAM, (International Food Policy Research Institute 2019, 2020)).

GEOS-Chem is a global atmospheric chemistry transport model that simulates the formation and fate of pollutants globally at a grid resolution of 2° × 2.5°, with 47 vertical levels (Bey *et al* 2001). The adjoint of the GEOS-Chem model calculates the sensitivity of a particular model response metric with respect to an emission perturbation in any of the global model 2 × 2.5° grid cells (Henze *et al* 2007), accounting for all of the mechanisms related to aerosol formation and fate. These sensitivities are output from the GEOS-Chem adjoint model as 'coefficients', which are then multiplied by emission estimates in each grid to estimate the change in the particular response metric associated with a given magnitude of emissions. The GEOS-Chem Adjoint model has been used to calculate, for 169 countries globally, coefficients that quantify the sensitivity of national, population-weighted PM<sub>2.5</sub> concentrations to changes in emissions in 2 × 2.5° grids globally (see Kuylenstierna *et al* (2020) for more details).

The health impacts attributable to ambient PM<sub>2.5</sub> exposure result from the overall total PM<sub>2.5</sub> from all sources. For consistency with existing global total PM<sub>2.5</sub>-attributable mortality estimates produced by the Global Burden of Disease (GBD), the population-weighted annual average PM<sub>2.5</sub> concentrations for each country was set to the values used in the GBD 2019 study (Health Effects Institute 2020, Murray *et al* 2020). The GEOS-Chem adjoint coefficients were then used to estimate the fraction of the total population-weighted PM<sub>2.5</sub> concentration for each country that resulted from agricultural emissions estimated in this study. To do this, the global gridded emissions from the agriculture sector were aggregated to the same 2 × 2.5° grids as the adjoint coefficients. Anthropogenic emissions from non-agricultural sources were taken from the EDGAR emissions database (Crippa *et al* 2018), and re-gridded to the same 2 × 2.5° grids. The product of the gridded PM<sub>2.5</sub> and PM<sub>2.5</sub>-precursor emissions and the set of coefficients for each country resulted in the estimated annual population-weighted PM<sub>2.5</sub> resulting from agricultural and non-agricultural sources. These values were then scaled by the ratio of the total population-weighted PM<sub>2.5</sub> from the GBD study, and the sum of GEOS-Chem adjoint-derived population-weighted PM<sub>2.5</sub> due to agricultural emissions, non-agricultural anthropogenic emissions, and natural background PM<sub>2.5</sub> concentrations (computed from GEOS-Chem forward model runs), to provide a consistent estimate of the agricultural contribution to the population-weighted PM<sub>2.5</sub> concentrations used to estimate global disease burdens in the GBD 2019 study (Murray *et al* 2020).

The health impacts attributable to PM<sub>2.5</sub> concentrations attributable to agricultural emissions were estimated for adults over 30 years for chronic obstructive pulmonary disease, ischemic heart disease, ischemic stroke, lung cancer, and Type 2 diabetes and for children less than 5 years for lower respiratory infections using equation 19. The relative risk (RR) corresponding to a given magnitude of total PM<sub>2.5</sub> exposure was derived from the Integrated Exposure Response (IER) functions developed for the GBD 2019 study, using the same theoretical minimum risk exposure level (uniform distribution between 2.4 and 5.9 μg m<sup>-3</sup>) (Murray *et al* 2020). The IER functions integrate results from epidemiological studies of ambient, household and second-hand smoke PM<sub>2.5</sub> exposure to derived functions that quantify the relative risk for each disease category across a wide range of PM<sub>2.5</sub> exposures. For each country, equation 19 was applied to estimate the premature mortality attributable to total PM<sub>2.5</sub> exposure, for each disease category. The fraction of national total population-weighted annual PM<sub>2.5</sub>

due to agricultural emissions was then used to estimate the fraction of the health burden attributable to agricultural emissions.

Once emitted, methane is globally mixed and contributes to background ozone. Exposure to ozone is associated with respiratory and cardiovascular mortality (Turner *et al* 2016). The contribution of methane emissions from agriculture to ozone concentrations, and associated respiratory and cardiovascular mortality, was calculated using results from the UN Environment Programme Global Methane Assessment (UNEP & CCAC 2021). In that study, a five model intercomparison was performed to characterize the response of ozone to methane emissions changes. The health impacts of the ozone changes were then evaluated using 2015 population and baseline mortality data and the exposure-response functions reported in a large epidemiological study using the American Cancer Society Cancer Prevention Study-II cohort of persons aged 30 years and over (Turner *et al* 2016). The ozone metric for which the response of changes in methane was characterised was national, population-weighted maximum daily 8h average ozone concentration, which is the ozone exposure metric used in the underlying epidemiological study (Turner *et al* 2016). These ozone-related impacts were found to vary nearly linearly with the size of the methane perturbation, so that the results can be interpolated to the methane emissions estimated for the agriculture sector in this work. However, the gradient of the linear relationship between methane changes and the ozone exposure metric and associated health impacts, varied between countries, due to differences in the levels of non-methane ozone precursors in different locations (i.e. levels of nitrogen oxides, non-methane volatile organic compounds, and carbon monoxide). In this study, the health burden from global agricultural methane emissions were estimated individually for each country using the country-specific linear relationships between methane emissions and ozone health impacts. We use the multi-model mean as our central estimate, with uncertainties encompassing both those in the physical response of ozone to methane changes from the multi-model analysis and those inherent in the exposure-response function. For further details see UNEP & CCAC (2021).

### 3. Results

#### 3.1. Air pollutant and greenhouse gas emissions from agriculture

In 2018, this study estimated that global agriculture emitted 129 million tonnes of methane, similar to previous study estimates (table 3, table 4). In the majority of regions, enteric fermentation from cattle contributed over 50% of total methane emissions from the agriculture sector, except east and south-east Asia, where rice production made the largest contribution (figure 2). For nitrous oxide, 4.4 million tonnes were emitted globally in 2018. This is approximately 25% lower than previous estimates (table 3), due to lower emissions from synthetic fertiliser application, and differences in N<sub>2</sub>O emissions from manure management, application and grazing (table 3). FAOSTAT estimates a substantially larger proportion of N<sub>2</sub>O emissions from grazing animals than from manure management and subsequent application, likely reflecting different assumptions regarding the types of manure management systems in place globally. The distribution of total N<sub>2</sub>O emissions across regions and countries was similar to those shown for methane (figure 2, emissions of all GHGs and pollutants, gridded at 0.083° resolution are shown in figure 3), while the contribution of subsectors varied, with larger contributions from grazing in Latin America and the Caribbean, and larger contributions of synthetic fertilisers application in South Asia, and East and South East Asia.

For air pollutants, the 44 million tonnes of ammonia emitted globally in 2018 mostly resulted from manure management and application. The distribution of ammonia emissions between countries and regions was similar to methane and N<sub>2</sub>O (figure 3), but compared to N<sub>2</sub>O, there were smaller contributions from grazing and synthetic fertiliser application (figure 2). Global ammonia emissions, and their spatial distribution were similar to previous estimates (table 3, figure 3). For nitrogen oxides, 8.6 million tonnes (expressed as mass units of NO<sub>2</sub>), were emitted in 2018, with synthetic fertiliser application the largest source (table 3; figure 2). This value is over 50% higher than NO<sub>x</sub> emissions estimated in EDGAR v5.0 and CEDS, which is consistent with underestimates in bottom-up inventories compared to total NO<sub>x</sub> emissions derived from remote-sensing observations (Elguindi *et al* 2020, Qu *et al* 2020). The burning of agricultural residues contributed the majority of the emissions of other pollutants, including particulate matter, black carbon, and non-methane volatile organic compounds, with a minor contribution from the diesel consumption from the use of machinery on farms (table 1). The EDGAR v5.0 inventory estimates higher emissions from agricultural burning compared to this study, as does the ECLIPSE v5a emissions, (3,848, and 337 kilotonnes of PM<sub>2.5</sub> and black carbon emissions in 2010, respectively) (Klimont *et al* 2017), which could reflect differences in the emission factors used for each pollutant used in ECLIPSE v5a compared to this study.

**Table 3.** Emissions of GHGs and air pollutants for FAO regions and globally from different sectors in agricultural sector in 2018 (units: kilotonnes, abbreviations: EE—Eastern Europe, ESEA—East and South East Asia, LAC—Latin America and the Caribbean, NA—North America, NENA—Near East and North Africa, OCE—Oceania, RUS—Russia, SA—South Asia, WE—Western Europe) and comparison with global datasets.

Pollutant	Source	EE	ESEA	LAC	NA	NENA	OCE	RUS	SA	SSA	WE	Global	Global—FAOStat (2018) <sup>a</sup>	Global—EDGAR v5 <sup>b</sup> (2015)	Global—CEDS (2018) <sup>c</sup>
CH <sub>4</sub>	Enteric fermentation	1606	9021	25878	7877	5506	2585	1135	18551	15412	6293	93865	99942	105692	
CH <sub>4</sub>	Manure management	194	3150	1334	891	303	73	112	1152	979	1117	9305	9864	12106	
CH <sub>4</sub>	Rice production	5	14408	724	0	79	7	19	7529	1976	62	24809	25348	36827	
CH <sub>4</sub>	Crop residue burning	0	458	246	0	0	0	0	346	114	0	1164	1049		
CH <sub>4</sub>	Total	1805	27039	28183	8769	5889	2666	1266	27579	18482	7472	129150	136203	154625	
N <sub>2</sub> O	Manure management	32	240	169	90	87	1	21	397	215	66	1318	452	390	
N <sub>2</sub> O	Manure application	29	272	110	81	31	2	16	104	99	87	831	611		
N <sub>2</sub> O	Graze	12	87	402	55	47	59	6	127	157	57	1010	2824		
N <sub>2</sub> O	Synthetic fertiliser	69	107	92	194	175	19	0	431	28	91	1206	2262		
N <sub>2</sub> O	Total	142	706	773	421	339	81	42	1059	500	302	4365	6149	5808	
NH <sub>3</sub>	Manure management	791	5811	2546	2702	1007	59	613	3352	2213	2511	21606		11594	20870
NH <sub>3</sub>	Manure application	367	3748	1326	1033	285	23	191	453	736	1170	9331			
NH <sub>3</sub>	Graze	62	426	1970	269	219	277	29	584	731	269	4837			
NH <sub>3</sub>	Synthetic fertiliser	245	742	446	881	1095	124	0	3164	119	335	7151		2513* (Urea only)	
NH <sub>3</sub>	Crop residue burning	0	407	219	0	0	0	0	308	101	0	1034		1415	
NH <sub>3</sub>	Total	1465	11134	6506	4885	2607	483	833	7861	3899	4285	43959		42115	45446
NO <sub>x</sub>	Manure management	35	265	123	104	53	2	30	199	118	70	1000		398	1168
NO <sub>x</sub>	Manure application	50	459	191	140	55	3	27	203	185	149	1461			
NO <sub>x</sub>	Graze	24	167	776	106	91	114	11	246	305	110	1949			
NO <sub>x</sub>	Synthetic fertiliser	143	223	191	403	364	40	0	895	57	190	2506			
NO <sub>x</sub>	Crop residue burning	0	387	199	0	0	0	0	297	91	0	974		1948	N.E.
NO <sub>x</sub>	Machinery diesel consumption	34	155	95	73	35	13	35	125	120	36	721			
NO <sub>x</sub>	Total	285	1656	1574	827	598	172	104	1965	876	554	8610		5450	5400
PM <sub>2.5</sub>	Crop residue burning	0	941	506	0	0	0	0	701	236	0	2384		3888	N.E.
PM <sub>2.5</sub>	Machinery diesel consumption	3	16	10	7	4	1	4	13	12	4	73			
PM <sub>2.5</sub>	Total	3	956	516	7	4	1	4	714	249	4	2458			
BC	Crop residue burning	0	91	51	0	0	0	0	66	24	0	232		363	N.E.
BC	Machinery diesel consumption	1	7	4	3	1	1	1	5	5	2	31			
BC	Total	1	98	55	3	1	1	1	71	30	2	263			
NMVOC	Crop residue burning	0	744	172	0	0	0	0	398	106	0	1419		3997	N.E.

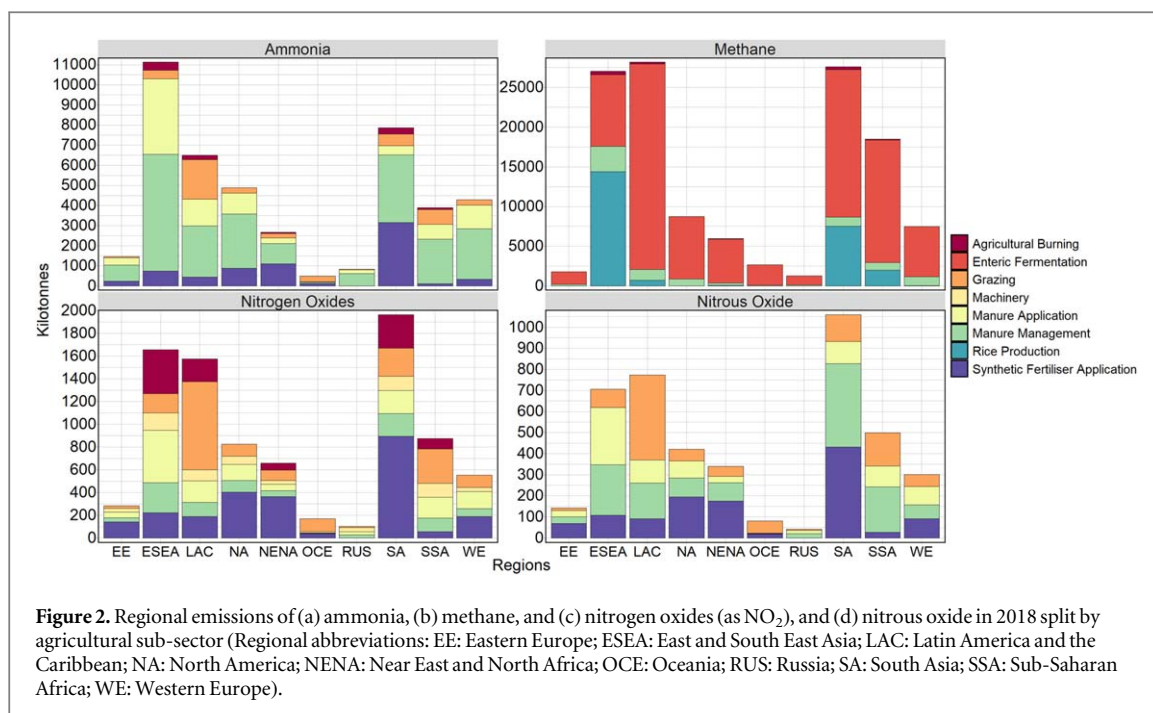
Table 3. (Continued.)

Pollutant	Source	EE	ESEA	LAC	NA	NENA	OCE	RUS	SA	SSA	WE	Global	Global—FAOStat (2018) <sup>a</sup>	Global—EDGAR v5 <sup>b</sup> (2015)	Global—CEDS (2018) <sup>c</sup>
NMVOC	Machinery diesel consumption	2	8	5	4	2	1	2	7	6	2	38			
NMVOC	Total	2	752	177	4	2	1	2	405	112	2	1458			

<sup>a</sup> <http://www.fao.org/faostat/en/#data><sup>b</sup> <https://edgar.jrc.ec.europa.eu/> (Crippa *et al* 2018)<sup>c</sup> (McDuffie *et al* 2020, O'Rourke *et al* 2020)

**Table 4.** Summary of global emissions (thousand tonnes), and annual premature mortality attributable to malnutrition, overweight/obesity, dietary and agricultural air pollution between 2014 and 2018.

Variable	2014	2015	2016	2017	2018
Agricultural methane emissions (kilotonnes)	123,887	124,876	126,912	128,131	129,150
Agricultural nitrous oxide emissions (kilotonnes)	4,089	4,221	4,205	4,357	4,365
Agricultural ammonia emissions (kilotonnes)	41,443	42,300	42,295	43,785	43,959
Agricultural nitrogen oxides emissions (kilotonnes)	8,108	8,367	8,309	8,679	8,610
Agricultural PM <sub>2.5</sub> emissions (kilotonnes)	2,494	2,528	2,535	2,649	2,458
Agricultural black carbon emissions (kilotonnes)	267	270	270	283	263
Agricultural volatile organic compounds emissions (kilotonnes)	1,443	1,448	1,454	1,509	1,458
Diet high in total red meat consumption (thousand premature deaths)	1,337 (1,089–1,585)	1,364 (1,109–1,620)	1,405 (1,140–1,669)	1,437 (1,167–1,707)	1,494 (1,215–1,773)
Diet low in fruits (thousand premature deaths)	1,017 (650.9–1,382)	1,025 (654.6–1,394)	1,044 (666.6–1,422)	1,033 (660.7–1,406)	999.6 (643–1,355)
Diet low in legumes (thousand premature deaths)	649.1 (289.1–1,009)	668.6 (298–1,039)	679.5 (303.8–1,055)	660.9 (296.1–1,026)	673.2 (301–1,046)
Diet low in milks (thousand premature deaths)	72.2 (36.6–107.8)	74.3 (35.8–112.8)	76.2 (36.2–116.3)	78.1 (37.0–119.2)	80.7 (38.6–122.8)
Diet low in vegetables (thousand premature deaths)	787.6 (307.5–1,268)	859.1 (341.4–1,377)	842.5 (329.3–1,356)	845.9 (331.2–1,361)	872.7 (3,409–1,405)
Maternal malnutrition (thousand premature deaths)	151	149.7	139.9	137.4	136.0
Moderate child stunting (thousand premature deaths)	199 (176–243)	194.8 (156.6–224.1)	184.6 (148.0–212.8)	177.0 (141.9–204.1)	170.4 (137.3–197.1)
Severe child stunting (thousand premature deaths)	485.8 (463.3–503.4)	517.6 (494.0–536.5)	484.0 (461.9–501.4)	452.2 (431.4–468.6)	423.7 (403.7–439.3)
Overweight (thousand premature deaths)	3,073 (1,575–4,571)	3,144 (1,599–4,688)	3,225 (1,643–4,806)	3,309 (1,686–4,932)	3,405 (1,747–5,064)
Obese (thousand premature deaths)	2,357 (1,556–3,158)	2,420 (1,592–3,249)	2,490.3 (1,640–3,341)	2,563 (1,692–3,433)	2,639 (1,745–3,534)
Ambient PM <sub>2.5</sub> due to agricultural emissions (thousand premature deaths)	524.4 (395.9–652.9)	534.1 (402.4–665.8)	522.5 (392.7–652.3)	529.0 (395.6–662.4)	536.8 (401.1–672.5)
Ambient PM <sub>2.5</sub> due to agricultural NH <sub>3</sub> emissions only (thousand premature deaths)	356.1 (268.8–443.4)	356.9 (268.9–444.9)	351.0 (263.8–438.2)	355.7 (266.0–445.4)	357.7 (267.3–448.1)
Ground-level ozone due to agricultural methane emissions (thousand premature deaths)	176.1 (75.7–228.9)	177.5 (76.3–230.8)	180.4 (77.6–234.5)	182.2 (78.3–236.9)	183.6 (78.9–238.7)



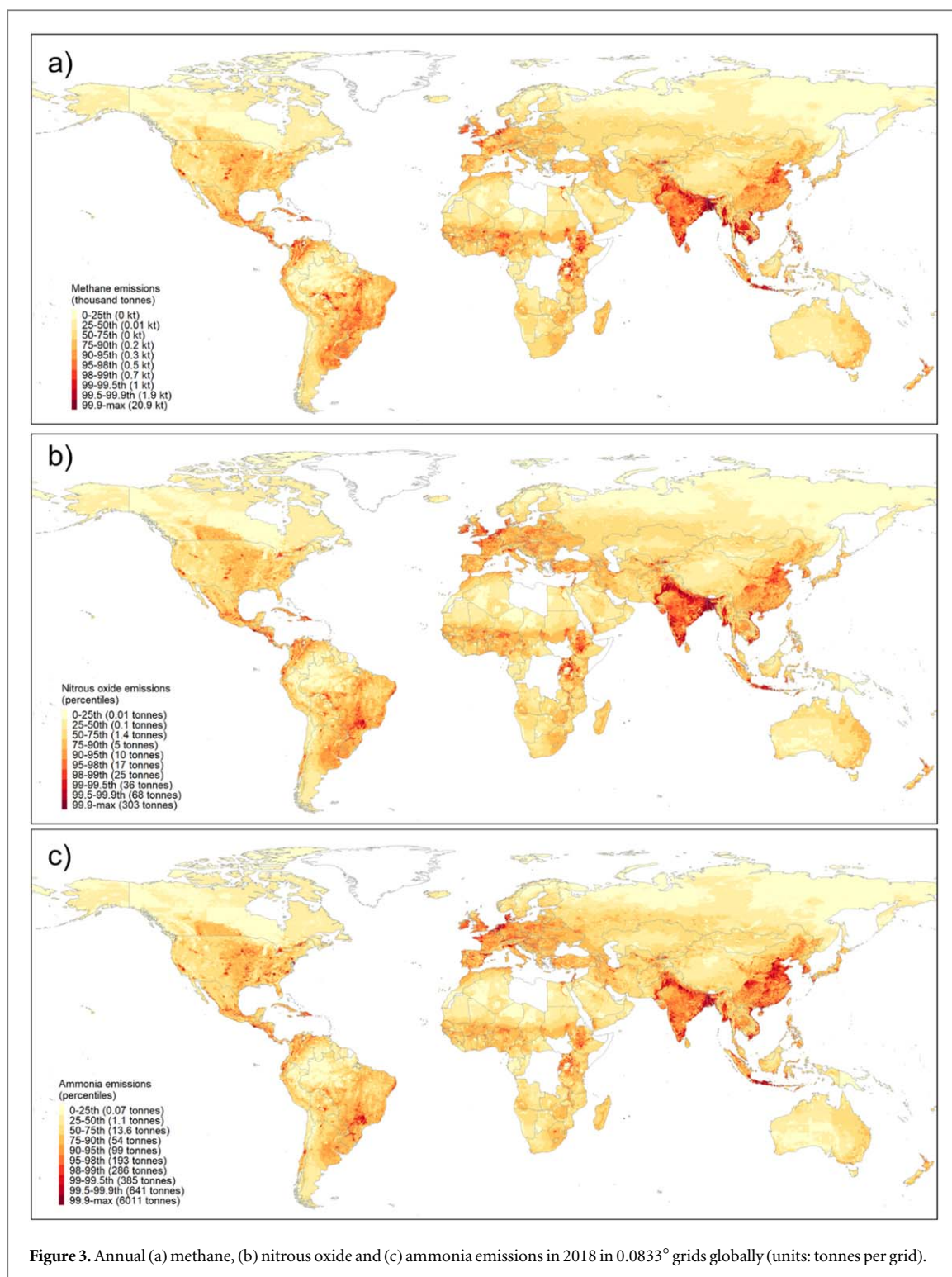
### 3.2. Human health impacts attributable to food and agricultural risk factors

The proportion of the population malnourished in each country in 2018 is shown in figure 4, and in 2018 was estimated to be approximately 809 million people, equivalent to 9% of the global population. This value is similar to the 8.9% of the global population estimated to be undernourished by FAO in 2017 (FAO *et al* 2020), which is expected since the FAO (2003) method was utilised in this study. Simultaneously, 43% of the global population were estimated to be overweight in 2017, and 14% were estimated to be obese, which is consistent with FAO (2020) that estimated 13.1% of the global population to be obese in 2016. The lowest levels of overweight and obesity were estimated for sub-Saharan Africa, and the highest levels in North America and Europe (figure 4). For dietary risks, 77% and 72% of the global population were estimated to consume below the minimum risk level of fruits and vegetables, respectively, and 66% of the global population consume more than the minimum risk level of red meat.

The largest health impact associated with dietary and food consumption risks was high body-mass index (overweight/obesity), with 3.4 million (overweight) and 2.6 million (obesity) premature deaths estimated for 2018 (table 5), and a 13 and 12% increase, respectively, since 2014 (table 4). The largest fraction of these premature deaths occurred in East and South-east Asia, followed by South Asia. Dietary risk factors including consumption of red meat, and diets low in fruits and vegetables contributed the next largest fraction of premature deaths, and were estimated to contribute to 4.1 million premature deaths in 2018. Different dietary risk factors made the largest contribution to this health burden in different regions. For example, the largest health burdens attributable to diets high in total red meat consumption were in Western and Eastern Europe, North America and East and South East Asia compared to the other dietary health risks (table 5). However, diets high in red meat made a relatively smaller contribution to dietary health risks in South Asia and Sub-Saharan Africa, where diets low in fruit and vegetables contributed a much higher fraction of the overall health burden from dietary risk factors.

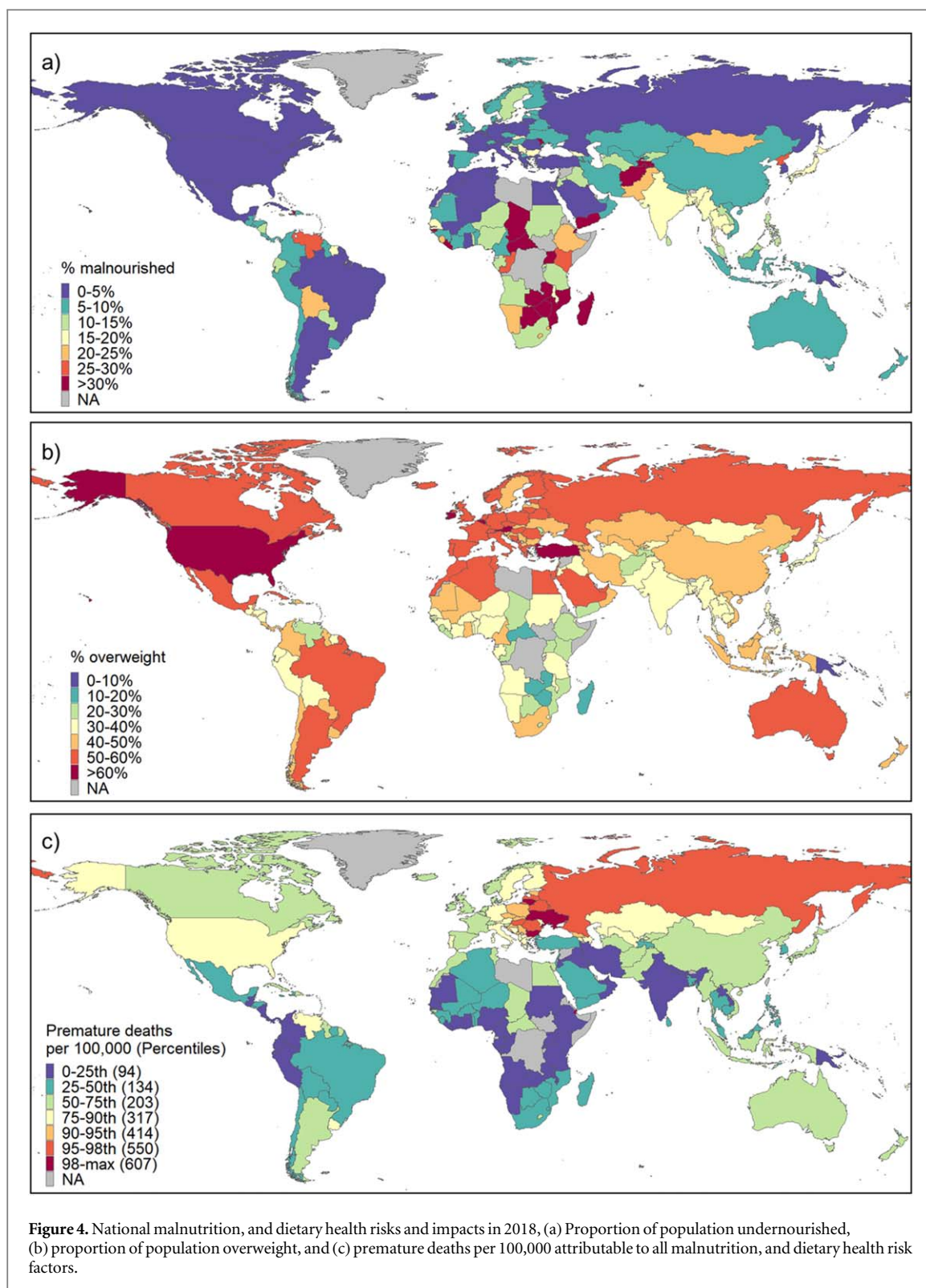
The health risks due to malnutrition combined to be attributable to over 700 thousand infant deaths in 2018, which predominantly occurred in sub-Saharan Africa and South Asia (table 5). This health impact is likely underestimated, as child stunting is only one metric to quantify child malnutrition. Other metrics, including child underweight (weight for age), and child wasting (low weight for height) have also been associated with health burdens. To avoid double counting, only child stunting was quantified in this analysis, but the Global Burden of Disease 2019 analysis estimated 1.2 million premature deaths were attributable to 'Child growth failure', which includes all three metrics (Murray *et al* 2020).

The highest mortality rates (premature deaths per 100,000) associated with the dietary, malnutrition and overweight/obesity risk factors considered were in Russia and Eastern Europe, followed by the United States and central Asian countries (figure 5). The premature deaths estimated for 2018 are generally comparable with those estimated in previous GBD studies (table 5). Health burdens from red meat consumption in this study were higher than those in the GBD 2017 and GBD 2019 studies as total red meat was the risk factor considered, compared to unprocessed red meat in the GBD study (processed red meat is included in the 'processed meat' risk



factor in GBD studies). The impacts on infant deaths attributable to maternal malnutrition are ~9% of the GBD 2019 estimate of the health burden from low birth weight, highlighting that maternal malnutrition is not the only contributor to infant deaths from low birth weight.

In addition to the dietary health impacts, the agricultural emissions described in section 3.1 were estimated to contribute between <5% up to 30% of the annual average national population-weighted  $PM_{2.5}$  concentrations, with the largest absolute contribution in China, followed by other South and East Asian countries (figure 4). The contribution of the agriculture sector to  $PM_{2.5}$  concentrations was consistent with previous studies for many regions (Karagulian *et al* 2017, Li *et al* 2017, Crippa *et al* 2019). For some regions, such as Latin America, and East Asia, the contribution of the agriculture sector to population-weighted  $PM_{2.5}$  was larger than in these previous studies. This may be due to underestimates in the EDGAR v5.0 emission inventory of non-agriculture emissions in these regions, which have been shown to be lower than other emission estimates



in Latin America (Huneus *et al* 2020), as well as differences in the representation of the chemical and physical processing of pollutant in the models used (e.g. Crippa *et al* (2019) use the TM5-FASST model to assess source sector contributions, compared to the GEOS-Chem Adjoint model used in this study).

Agricultural emissions were estimated to result in 537 thousand premature deaths in 2018 due to their contribution to ambient  $PM_{2.5}$  concentration globally (table 5, figure 6), equivalent to 13% of total premature deaths attributable to ambient  $PM_{2.5}$  exposure, and an additional 184 thousand premature deaths from the formation of ground-level ozone from agricultural methane emissions. Both the agricultural  $PM_{2.5}$  and ozone premature deaths occurred mostly in China and South Asia (table 5), which also had among the highest premature death rate from air pollution due to agricultural emissions, alongside Eastern European countries

**Table 5.** Premature deaths associated with food and agricultural risk factors for FAO regions and globally in 2018 (units: thousand people, abbreviations: EE—Eastern Europe, ESEA—East and South East Asia, LAC—Latin America and the Caribbean, NA—North America, NENA—Near East and North Africa, OCE—Oceania, RUS—Russia, SA—South Asia, WE—Western Europe).

Risk	EE	ESEA	LAC	NA	NENA	OCE	RUS	SA	SSA	WE	Global	GBD 2017	GBD 2019
Diet high in total red meat consumption	119.6	640.0	121.3	185.5	55.2	11.3	105.7	13.1	14.1	228.2	1494 (1215–1773)	24.8	850.5 <sup>a</sup>
Diet low in fruits	79.7	213.5	45.7	49.9	43.1	5.7	77.0	338.2	95.2	51.6	999.6 (643–1355)	2423.4	1008.1
Diet low in legumes	63.9	277.3	16.0	45.8	62.0	3.6	59.0	59.8	17.6	68.1	673.2 (301–1046)	534.8	1067.1
Diet low in milks	1.1	58.8	5.0	0.2	2.4	0.1	1.1	6.6	4.4	1.0	80.7 (38.6–122.8)	126.1	154.7
Diet low in vegetables	25.5	146.6	106.7	55.6	28.3	5.0	59.8	289.8	83.2	72.2	872.7 (3409–1,405)	1462.4	508.7
Maternal malnutrition	0.0	5.8	2.1	0.1	3.5	0.0	0.0	59.4	65.0	0.1	136.0		1833.2 <sup>b</sup>
Moderate child stunting	0.5	11.5	0.0	1.2	9.1	0.5	0.6	62.7	83.5	0.8	170.4 (137.3–197.1)		
Severe child stunting	0.0	36.0	48.0	0.0	6.4	0.8	0.0	106.2	226.4	0.0	423.7 (403.7–439.3)		1212.1 <sup>c</sup>
Overweight	213.2	1233.3	232.6	258.9	265.0	13.0	199.5	517.4	124.8	347.5	3,405 (1,747–5,064)		
Obese	152.5	916.8	214.5	241.2	212.3	10.4	142.0	365.0	89.2	295.4	2,639 (1,745–3,534)		4683.2 <sup>d</sup>
Ambient PM <sub>2.5</sub> due to agricultural emissions	13.5	298.0	27.2	3.2	8.6	0.1	5.6	159.8	4.1	16.8	536.8 (401.1–672.5)		
Ambient PM <sub>2.5</sub> due to agricultural NH <sub>3</sub> emissions only	8.8	262.5	22.3	2.9	5.0	0.0	4.9	36.9	1.4	13.2	357.7 (267.3–448.1)		
Ground-level ozone due to agricultural methane emissions	8.2	57.7	9.7	10.8	14.0	0.5	6.3	50.3	10.2	15.9	183.6 (78.9–238.9)		

<sup>a</sup> Unprocessed red meat consumption only

<sup>b</sup> Total health burden attributable to low birth weight

<sup>c</sup> Premature deaths attributable to Child Growth Failure

<sup>d</sup> Premature deaths attributable to high body mass index (i.e. combined overweight and obese)

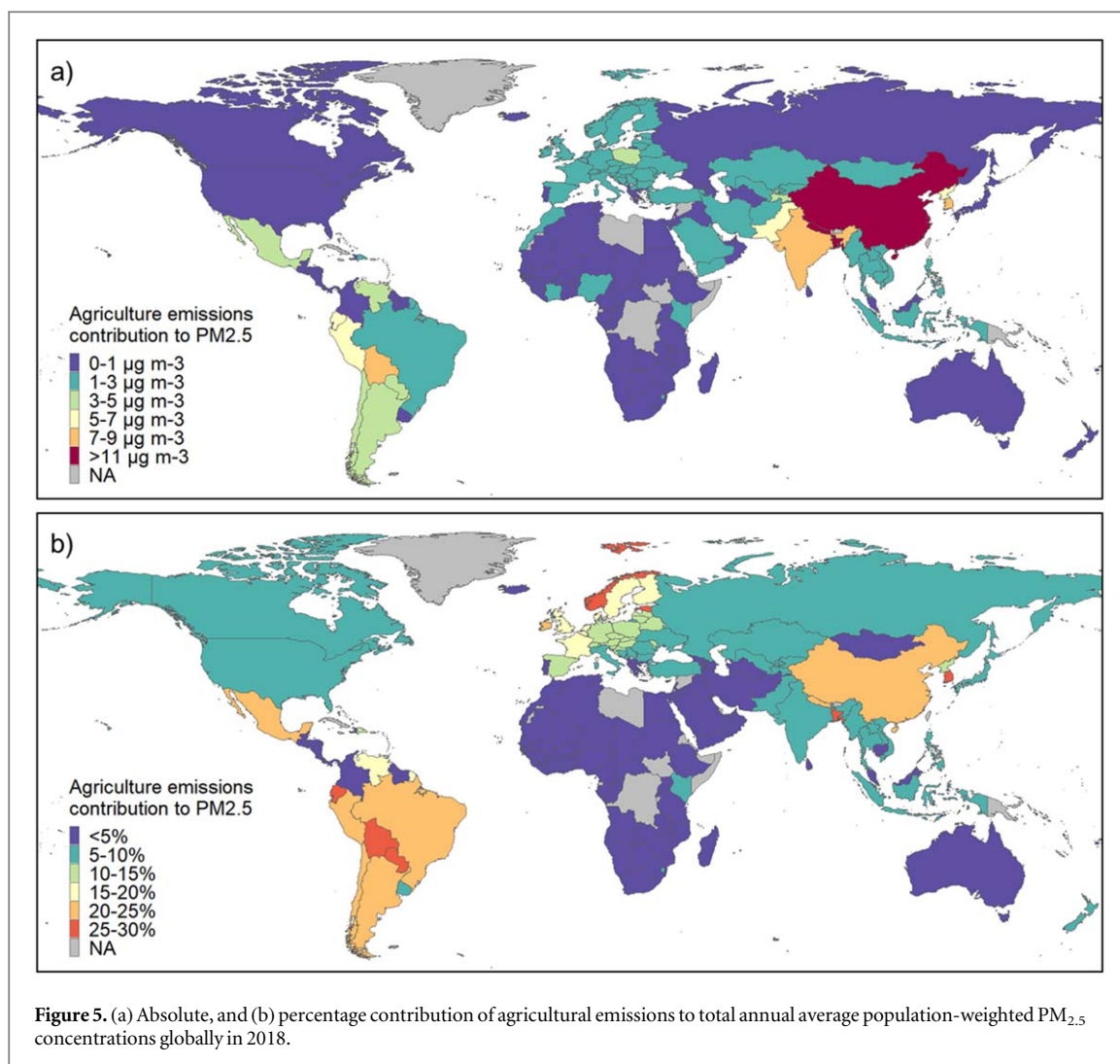


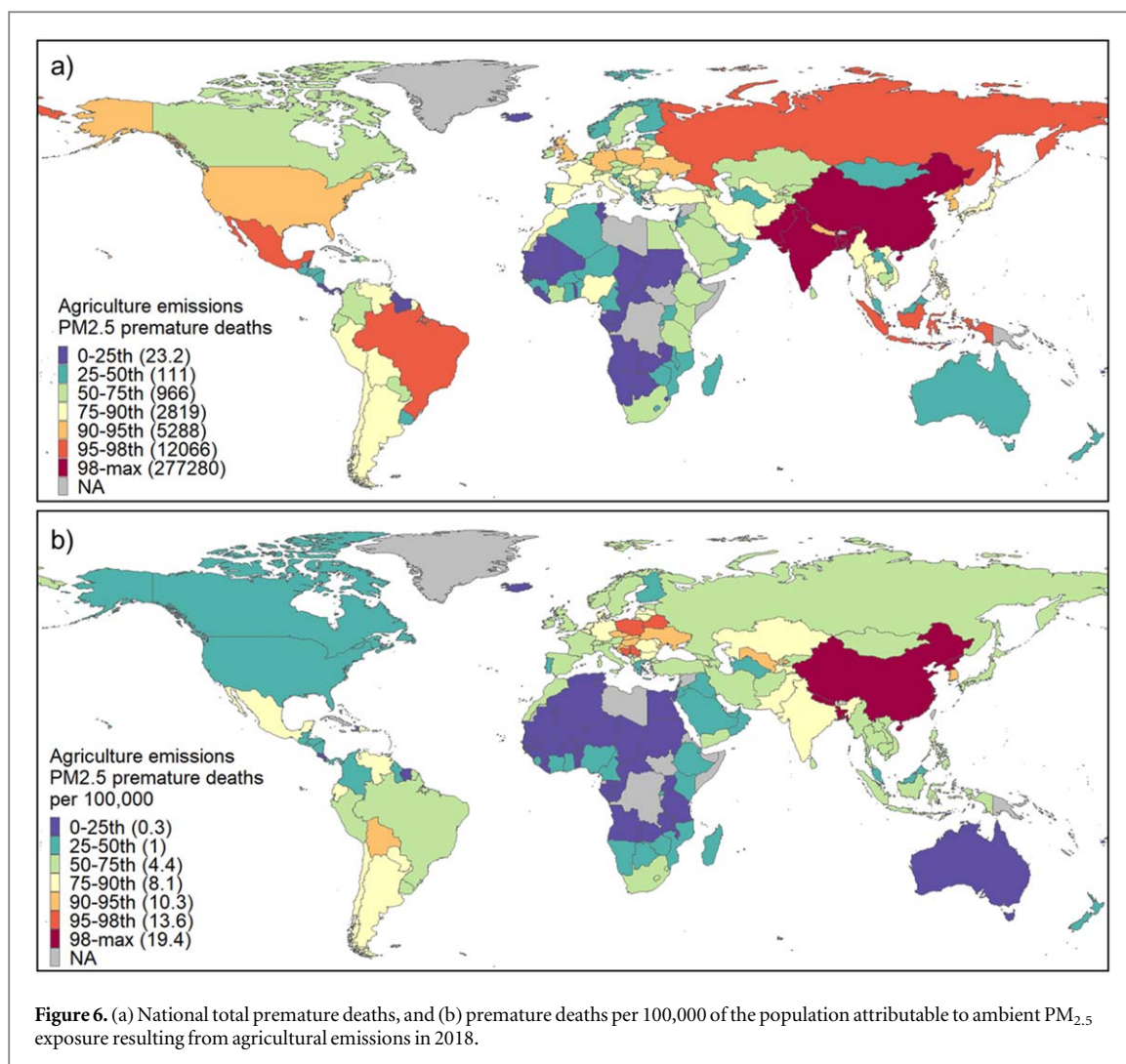
(figure 6). The absolute PM<sub>2.5</sub> health burden from agricultural emissions estimated in this study is 18% smaller than those estimated Lelieveld *et al* (2015) (650 thousand premature deaths in 2010), which may be due to differences in the categories considered in the agriculture sector, as well as methodological differences such as the different concentration-response functions used.

Two-thirds of the global health impact attributable to PM<sub>2.5</sub> resulting from agricultural emissions was from agricultural ammonia emissions (358 thousand premature deaths in 2018, 9% of the total PM<sub>2.5</sub>-attributable mortality) (table 5). The proportion of agricultural PM<sub>2.5</sub> health impacts due to ammonia emissions was highest in North America (90%), East and South East Asia (88%), Western Europe (79%), and Latin America and the Caribbean (82%). However, in South Asia, only 23% of PM<sub>2.5</sub>-attributable premature deaths due to agricultural emissions were due to ammonia emissions (table 5), with other sources, specifically agricultural residue burning, making a larger contribution.

## 4. Discussion

### 4.1. Implications for evaluating integrated strategies in the agriculture sector

Agricultural systems play a crucial role in achieving food and nutritional security, as well as in economic growth and rural development. At the same time, agriculture can also result in a range of environmental impacts, as well as impacts on human health, indirectly through food consumption (or lack thereof) or directly through the air pollutant emissions emitted from agricultural activities. These impacts have often been assessed separately. The modelling framework presented in this work has integrated the assessment of dietary, and air pollution health risks, with the contribution of the agriculture sector to climate change. When applied to the years 2014–2018, the model produces broadly comparable results to previous global estimates of GHG emissions, and health burdens from dietary risks, malnutrition and obesity/overweight that are estimated independently. The ability



to integrate assessment of health, air pollution and climate impacts of food production and consumption has several implications for the evaluation of integrated strategies to mitigate these impacts.

A variety of mitigation actions can reduce the contribution of agriculture to climate change, including (i) technical measures on-farms such as feed optimisation, improvements to manure management systems, improving animal husbandry, and intermittent aeration of rice paddy fields (FAO 2013, Gerber *et al* 2013), (ii) shifting diets to reduce consumption of high-GHG emitting foods, such as red meat, and (iii) reducing food waste (FAO 2019). Shifting diets to lower GHG-emitting food products has been linked with additional health benefits previously (Springmann *et al* 2016a, 2017, 2018, Clark *et al* 2019, Willett *et al* 2019). This study is consistent with previous studies in estimating a substantial health burden from red meat consumption (1.5 million premature deaths in 2018), highlighting the considerable health benefits that could be achieved alongside reductions in greenhouse gases from reducing total red meat consumption.

Moreover, this study quantifies the additional health benefits, from reductions in agricultural air pollutant emissions, achievable from shifting diets, and from other agricultural climate change mitigation strategies that do not necessarily affect exposure to dietary health risks (i.e. on-farm technical measures and reductions in food waste). Reductions in methane, in addition to mitigating climate change, will also reduce background surface ozone concentrations, while reducing ammonia emissions, alongside co-emitted GHGs like N<sub>2</sub>O from manure and synthetic fertilisers will also reduce premature deaths associated with PM<sub>2.5</sub> exposure. The ~700,000 annual premature deaths estimated in this study from air pollutants from agricultural emissions may underestimate the health benefits that could be achieved from agricultural emission reduction strategies. Firstly, non-fatal health outcomes associated with air pollution exposure, such as asthma incidence and exacerbations (Anenberg *et al* 2018), and non-fatal cardiovascular diseases (REVIHAAP, 2013), have not been quantified. Secondly, for some climate change mitigation actions, additional reduction in air pollutant emissions may occur in other sectors, which have not been considered in this study. For example, reducing food waste could also avoid methane and ammonia emissions from the decomposition of organic waste at solid landfill sites (Tonini *et al* 2018). There are

also additional health burdens (and possible benefits) from other dietary risk factors not quantified in this study, including diets low in whole grains (GBD 2017 Diet Collaborators, 2019). Finally, other health impacts associated with food consumption were also not quantified, such as foodborne diseases, e.g. diarrhoeal disease agents, which was previously estimated to be associated with approximately 420 thousand premature deaths in 2010 (WHO 2015).

Possible trade-offs are also highlighted between different health and environmental considerations in the development of agricultural strategies. For example, many, particularly low and middle-income, countries have developed agricultural strategies that aim to intensify or extensify agricultural production, as one action among many other options, to alleviate poverty, and increase economic growth (Zimmermann *et al* 2009, Brüntrup 2011, Kolavalli *et al* 2013). Reducing malnutrition and exposure to dietary risks could yield substantial health benefits in reducing child and adult mortality. However, achieving these benefits could have implications for food production, and associated impacts. For malnutrition, and associated health impacts, there are a large number of drivers (Gillespie and van den Bold 2017). Domestic food production systems, included in this modelling framework, can influence the prevalence of malnutrition and food availability due to a shortage in the availability of grains or other staples (FMARD 2016), and from transitions to different food production systems (Gillespie and van den Bold 2017). In addition, policies to increase food production or change food production systems which are specifically designed to improve health and reduce malnutrition have been identified, including increasing household agricultural production (Gillespie and van den Bold 2017, Wendt *et al* 2019), developing more diverse production systems, and improving the productivity of nutrient dense food products (Headey *et al* 2012, Gillespie and van den Bold 2017). However, there are a substantial number of other factors that influence food availability and the prevalence of malnutrition, including income levels, non-food expenditures, women's employment etc (Gillespie and van den Bold 2017). These factors are not explicitly included in the modelling framework presented in this work, which is consistent with similar models developed previously to assess the link between agricultural production under different future climate scenarios and the prevalence of malnutrition (Dawson *et al* 2016). More detailed conceptual frameworks have been developed to characterise the links across the wider drivers of malnutrition (Gillespie *et al* 2012, Headey *et al* 2012). The application of this modelling framework to assess future scenarios for agricultural development allows assessment of the consequences of different scenarios on dietary, obesity and malnutrition health risks, alongside any trade-offs that occur due to intensification (e.g. resulting in increased inorganic fertiliser application, increased livestock numbers etc), extensification or other changes to agricultural systems, e.g. to achieve dietary or health goals. In addition, trade-offs between emissions of GHGs and air pollution from different on-farm mitigation options (e.g. differential effects of mitigation options for manure management between methane and nitrous oxide and ammonia emissions, as outlined in Sajeev *et al* (2018)) can also be assessed.

There are also trade-offs in the quantification of health and climate impacts of food production and consumption in this integrated model, as compared to developing separate and independent estimates of these indicators. As noted above, the estimated health burdens from dietary health risks and malnutrition are not as comprehensive as in studies that estimates these impacts in isolation, such as the Global Burden of Disease (GBD 2017 Diet Collaborators 2019). For example, the exposure to specific dietary risks cannot be estimated directly from food balances, underestimating the overall health burden from dietary risks. Examples of the dietary risks which could not be integrated into the modelling framework presented here include those that are associated with processed foods such as diets high in processed meat, and diets high in sugar sweetened beverages, and diets low in whole grains, which are not disaggregated in FAO food balances from other food consumption (i.e. processed and unprocessed red meat, sugar sweetened beverages and other sugar consumption and whole and refined grains). Finally, for estimation of GHG and air pollutant emissions, the modelling framework presented here quantifies those emissions that occur due to activities on the farm. Other modelling tools which focus solely on GHG emissions in the agriculture sector, such as the GLEAM tool (FAO 2018), also provide estimates of GHG emissions from pre- and post-farm processes, such as fertiliser production.

#### 4.2. Limitations, uncertainties and future development

The first limitation of the modelling is that the emissions occurring within national borders are those assigned to a country. The health impacts, both from dietary and air pollution risk factors, are those occurring to the national population. The dietary health impacts result from the consumption of foods produced domestically and those that are imported from other countries. In addition, the agricultural air pollution health impacts for a population result both from agricultural emissions occurring within the country, and from agricultural emissions in other countries that are transported in the atmosphere across borders. In this study, the agricultural GHG and air pollutant emissions associated with the production of food that is imported into a particular country is accounted for in the emission total for the producer country. This is consistent with international GHG and air pollution emission accounting and reporting frameworks (IPCC 2006, EMEP/EEA 2019), and does not affect the estimated emissions or health impacts quantified for 2014–2018. However, previous studies

have assessed the impact of global trade on air pollution health impacts (Zhang *et al* 2017), and future work to integrate international trade into the modelling framework, would allow the implications of changes in diets in one country on the GHG and air pollutant emissions (and associated health impacts) in the producer country, to be quantified.

In addition, the modelling framework draws its boundary at emission sources on the farm, in contrast to other models, such as GLEAM, which account for emissions from inputs and post-processing (FAO 2018). Other food production processes also contribute to emissions, including synthetic fertiliser production, and post-farm transport, processing, and food waste management (Tonini *et al* 2018, Walling and Vaneckhaute 2020). These emissions are categorised in other source categories in IPCC and EMEP/EEA source categories, and were therefore not included in this modelling framework (IPCC 2006, EMEP/EEA 2019). However, their future inclusion in the model would allow the impact of different mitigation strategies on all emissions impacted by changes in agricultural systems to be assessed.

Other limitations include the estimation of annual air pollutant emissions with no intra-annual disaggregation. The contribution of agricultural emissions to PM<sub>2.5</sub> concentrations varies across the year as emissions of ammonia and nitrogen oxides from manure management, application and grazing, as well as synthetic fertiliser application, and emissions from agricultural residue burning have pronounced seasonal cycles (Pinder *et al* 2006, Paulot *et al* 2014, Warner *et al* 2016, Wang *et al* 2018). The metric used to quantify health burdens in this study was the annual average PM<sub>2.5</sub> concentration, as long-term PM<sub>2.5</sub> exposure is more comprehensive for quantifying the overall PM<sub>2.5</sub> health burden compared to short-term exposure (REVIHAAP 2013). The impact of different temporal profiles of ammonia emissions on PM<sub>2.5</sub> concentrations were assessed across Europe, showing a 12% difference in annual average concentrations for different temporal profiles (Backes *et al* 2016). This indicates that the temporal profile of agricultural emissions does not introduce large uncertainties in the overall PM<sub>2.5</sub> health burden from long-term exposure. In addition, the assessment of PM<sub>2.5</sub> concentrations and health burdens does not include the contribution of secondary organic aerosol formation to total annual PM<sub>2.5</sub> concentrations, which has been associated with approximately 10% of the global air pollution health burden (Nault *et al* 2020).

In addition to the simplifications made for modelling agricultural systems and impacts on human health and climate, data and assumptions were extrapolated to develop a global assessment. For some agricultural emissions, e.g. livestock methane and nitrous oxide emissions, and methane emissions from rice, regional data on the livestock and rice growing seasons could be used to increase the specificity of the analysis. However, for other variables, including ammonia emissions from manure and inorganic fertiliser application, emission factors derived from the EMEP/EEA (2019) air pollution guidebook were used due to lack of data on local emission factors. This is consistent with earlier assessments that have used previous iterations of the EMEP/EEA emission inventory guidebooks to quantify agricultural emissions in regions that lack local data on specific variables (Castesana *et al* 2018, Crippa *et al* 2018). There are a limited number of studies that have assessed the transferability of EMEP/EEA emission factors to other regions, but a recent study of ammonia emissions from cattle in tropical and subtropical pastures measured emission factors that were consistent with EMEP/EEA (2019) (Arndt *et al* 2020).

Due to a lack of country or region-specific information, in undertaking the health impact assessment for dietary, obesity, malnutrition and air pollution health risks, dose-response functions developed in studies conducted in one region were applied to populations in other regions. This assumes that population globally respond similarly to particular exposures of health risks (e.g. the same magnitude of PM<sub>2.5</sub> or ozone air pollution exposure, or the same level of fruit or meat consumption). The dose-response functions used have been applied previously to quantify global health risks or are based on international assessments and reviewed that have identified the most appropriate global dose-response functions (Murray *et al* 2020). As studies on different health risks are conducted in different regions, these dose-response relationships can be updated to reflect regional differences in health responses.

## 5. Conclusions

Food production and consumption play a key role in climate change and human health through emissions of air pollutants, and dietary, malnutrition and obesity health impacts. The quantification of health benefits associated with the implementation of climate change mitigation measures has been put forward as a potential factor to increase climate change mitigation ambition, and to build a broad coalition of support for implementation (Linnér *et al* 2012, Shindell *et al* 2017). This work presents a new model that integrates the assessment of food consumption-related health risks, with quantification of the greenhouse gas emissions, and air pollutant emissions and health burden associated with food production. The application of this model to 2014–2018 estimates that there are annually approximately 6 million premature deaths associated with high body-mass index, over 4 million premature deaths associated with dietary health risks, and over 700 thousand infant deaths

associated with malnutrition. In addition, the emissions of PM<sub>2.5</sub>-precursor air pollutants, and methane from agriculture globally is associated with over 700 thousand premature deaths per year. The substantial health burdens associated with food consumption, in addition to those from emissions during its production on farms highlights the importance of developing integrated agricultural strategies that consider health and environmental impacts, and the importance of models that can assess their synergies and trade-offs.

## Acknowledgments

The authors are grateful to the Stockholm Environment Institute Integrated Climate and Development Planning initiative for funding this work. W.K.H. acknowledges the Science and Technology Facilities Council (STFC) for funding (Project Number: ST/V002481/1). The views and opinions expressed in this article are those of the authors and do not necessarily reflect the official policy or position of any agency. C S M is grateful to Guozhong Wang for guidance and advice on programming and coding. The open-source model presented in this work is available at: <https://github.com/chmalle41/aghealth>.

## Data availability statement

No new data were created or analysed in this study.

## ORCID iDs

Christopher S Malley  <https://orcid.org/0000-0001-5897-9977>

W Kevin Hicks  <https://orcid.org/0000-0002-9568-4606>

Jason Veysey  <https://orcid.org/0000-0001-8890-7704>

Drew T Shindell  <https://orcid.org/0000-0001-9925-8500>

Daven K Henze  <https://orcid.org/0000-0001-6431-4963>

Susan C Anenberg  <https://orcid.org/0000-0002-9668-603X>

## References

- Abbatati C *et al* 2020 Global burden of 369 diseases and injuries in 204 countries and territories, 1990–2019: a systematic analysis for the global burden of disease study 2019 *Lancet* **396** 1204–22
- Anenberg S C *et al* 2018 Estimates of the global burden of ambient PM<sub>2.5</sub>, ozone, and NO<sub>2</sub> on asthma incidence and emergency room visits *Environ. Health Perspect.* **126**
- Arizpe N, Giampietro M and Ramos-Martin J 2011 Food security and fossil energy dependence: an international comparison of the use of fossil energy in agriculture (1991–2003) *CRC. Crit. Rev. Plant Sci.* **30** 45–63
- Arndt C, Misselbrook T H, Vega A, Gonzalez-Quintero R, Chavarro-Lobo J A, Mazzetto A M and Chadwick D R 2020 Measured ammonia emissions from tropical and subtropical pastures: a comparison with 2006 IPCC, 2019 Refinement to the 2006 IPCC, and EMEP/EEA (European monitoring and evaluation programme and european environmental agency) inventory estimates *J. Dairy Sci.* **103** 6706–15
- Backes A, Aulinger A, Bieser J, Matthias V and Quante M 2016 Ammonia emissions in Europe, part I: Development of a dynamical ammonia emission inventory *Atmos. Environ.* **131** 55–66
- Bey I, Jacob D J, Yantosca R M, Logan J A, Field B D, Fiore A M, Li Q B, Liu H G Y, Mickley L J and Schultz M G 2001 Global modeling of tropospheric chemistry with assimilated meteorology: Model description and evaluation *J. Geophys. Res.-Atmos.* **106** 23073–95
- Blössner M, De Onis M and Organization, W. H. 2005 Malnutrition: quantifying the health impact at national and local levels *Environ. Burd. Dis. Ser.* **178** 293–304
- Brüntrup M 2011 The comprehensive Africa agriculture development programme (CAADP) - an assessment of a Pan-African attempt to revitalise agriculture - Q. *J. Int. Agric.*
- Castesana P S, Dawidowski L E, Finster L, Gómez D R and Taboada M A 2018 Ammonia emissions from the agriculture sector in Argentina; 2000–2012 *Atmos. Environ.* (<https://doi.org/10.1016/j.atmosenv.2018.02.003>)
- CCAC SNAP 2019 Opportunities for increasing ambition of nationally determined contributions through integrated air pollution and climate change planning: a practical guidance document *Climate and Clean Air Coalition Supporting National Action & Planning Initiative Repo*
- Clark M A, Springmann M, Hill J and Tilman D 2019 Multiple health and environmental impacts of foods *Proc. Natl. Acad. Sci. U. S. A.* **116** 23357–62
- Crippa M *et al* 2018 Gridded emissions of air pollutants for the period 1970–2012 within EDGAR v4.3.2 *Earth Syst. Sci. Data.* **10** 1987–2013
- Crippa M, Janssens-Maenhout G, Guizzardi D, Van Dingenen R and Dentener F 2019 Contribution and uncertainty of sectorial and regional emissions to regional and global PM<sub>2.5</sub> health impacts *Atmos. Chem. Phys.* **19** 5165–86
- Dawson T P, Perryman A H and Osborne T M 2016 Modelling impacts of climate change on global food security *Clim. Change* **134** 429–40
- Electric C, Raskin P, Rosen R and Stutz J 2009 The Century Ahead: Four Global Scenarios. Technical Documentation. Tellus Institute Report. Available at: (<https://www.polestarproject.org/publications.html>)
- Elguindi N *et al* 2020 Intercomparison of magnitudes and trends in anthropogenic surface emissions from bottom-up inventories, top-down estimates, and emission scenarios *Earth's Futur.* **8** 1–20
- EMEP/EEA 2019 Air pollutant emission inventory guidebook 2019 *EMEP/EEA Air Pollution Emission Inventory Guidebook 2019* -

- FAO 2019 *Five Practical Actions Towards Low-Carbon Livestock*. (Rome: Food and Agricultural Organization of the United Nations Report) Available at: (<http://www.fao.org/3/ca7089en/ca7089en.pdf>)
- FAO 2018 Global Livestock Environmental Assessment Model: Model Description Version 2.0. Food and Agricultural Organisation of the United Nations (FAO) report. Available at: ([http://www.fao.org/fileadmin/user\\_upload/gleam/docs/GLEAM\\_2.0\\_Model\\_description.pdf](http://www.fao.org/fileadmin/user_upload/gleam/docs/GLEAM_2.0_Model_description.pdf))
- FAO 2016 The agriculture sectors in the intended nationally determined contributions: analysis ed R Strohmaier *et al* *Environment and Natural Resources Management Working Pap.*
- FAO 2013 Mitigation of Greenhouse Gas Emissions in Livestock Production: A review of technical options for non-CO<sub>2</sub> emissions. FAO Animal Production and Health paper. ISSN: 0254-6019. Available at: (<http://www.fao.org/3/i3288e/i3288e.pdf>)
- FAO 2011 Energy-smart food for people and climate. FAO Issue paper. Available at: (<http://www.fao.org/docrep/014/i2454e/i2454e00.pdf>)
- FAO 2003 Keynote paper: FAO methodology for estimating the prevalence of undernourishment, in: Measurement and Assessment of Food Deprivation and Undernutrition: International Scientific Symposium Rome, 26–28 June 2002
- FAO/IFAD/UNICEF/WFP/WHO 2020 The state of food security and nutrition in the world 2020. transforming food systems for affordable healthy diets *IEEE Journal of Selected Topics in Applied Earth Observations and Remote Sensing*
- FMARD 2016 The Agriculture Promotion Policy (2016–2020): Building on the Successes of the ATA, Closing Key Gaps. Federal Ministry of Agriculture and Rural Development Policy and Strategic Document. Available at: (<http://nssp.ifpri.info/files/2017/12/2016-Nigeria-Agri>)
- Fowler D *et al* 2015 Effects of global change during the 21st century on the nitrogen cycle *Atmos. Chem. Phys.* **15** 13849–93
- GBD 2017 Diet Collaborators 2019 1958–1972 Health effects of dietary risks in 195 countries: a systematic analysis for the Global Burden of Disease Study 2017(2019) *The Lancet*, 393 (10184)
- Geddes J A and Martin R V 2017 Global deposition of total reactive nitrogen oxides from 1996 to 2014 constrained with satellite observations of NO<sub>2</sub> columns *Atmos. Chem. Phys.* **17** 10071–91
- Gerber P J *et al* 2013 Technical options for the mitigation of direct methane and nitrous oxide emissions from livestock: a review *Animal*. **220–34**
- Gilbert M, Nicolas G, Cinardi G, Van Boeckel T P, Vanwambeke S O, Wint G R W and Robinson T P 2018 Global distribution data for cattle, buffaloes, horses, sheep, goats, pigs, chickens and ducks in 2010 *Sci. Data.* **5** 180227
- Gillespie S, Harris J and Kadiyala S 2012 The agriculture–nutrition disconnect in india what do we know? *IFPRI Discuss. Pap.* **1187** 1–56
- Gillespie S and van den Bold M 2017 Agriculture, food systems, and nutrition: meeting the challenge *Glob. Challenges* **1** 1600002
- Headey D, Chiu A and Kadiyala S 2012 Agriculture’s role in the indian enigma: help or hindrance to the crisis of undernutrition? *Food Secur.* **4** 87–102
- Health Effects Institute 2020 State of Global Air 2020. Data source: Global Burden of Disease Study 2019. IHME, 2020
- Henze D K, Hakami A and Seinfeld J H 2007 Development of the adjoint of GEOS-Chem *Atmos. Chem. Phys.* **7** 2413–33
- Huneeus N *et al* 2020 Evaluation of anthropogenic air pollutant emission inventories for South America at national and city scale *Atmos. Environ.* **235** 117606
- International Food Policy Research Institute 2020 Spatially-Disaggregated Crop Production Statistics Data in Africa South of the Sahara for 2017 (<https://doi.org/10.7910/DVN/FSSKBW>), Harvard Dataverse, V2
- International Food Policy Research Institute 2019 Global spatially-disaggregated crop production statistics data for 2010 version 2.0 (<https://doi.org/10.7910/DVN/PRFF8V>), Harvard Dataverse, V4
- IPCC 2019a Climate change and land - summary for policymakers (draft) *Intergovernmental Panel on Climate Change Special Report on climate change, desertification, land degradation, sustainable land management, food security, and greenhouse gas fluxes in terrestrial ecosystems*
- IPCC 2019b Task force on national greenhouse gas inventories *Intergov. Panel Clim. Chang.*
- IPCC 2006 Guidelines for national greenhouse gas inventories *Agric. For. other L. use.* ([http://www.ipcc-nggip.iges.or.jp/public/2006gl/pdf/2\\_Volume2/V2\\_3\\_Ch3\\_Mobile\\_Combustion.pdf](http://www.ipcc-nggip.iges.or.jp/public/2006gl/pdf/2_Volume2/V2_3_Ch3_Mobile_Combustion.pdf))
- Karagulian F *et al* 2017 Attribution of anthropogenic PM<sub>2.5</sub> to emission sources. A global analysis of source-receptor model results and measured source-apportionment data., European Commission JRC Technical Reports
- Klimont Z, Kupiainen K, Heyes C, Purohit P, Cofala J, Rafaj P, Borken-Kleefeld J and Schöpp W 2017 Global anthropogenic emissions of particulate matter including black carbon *Atmos. Chem. Phys.* **17** 8681–8723
- Kolavalli S, Birner R and Flaherty K 2013 The comprehensive Africa agriculture program as a collective institution *SSRN Electron. J.* (<https://doi.org/10.2139/ssrn.2197400>)
- Kuylenstierna J C I *et al* 2020 Development of the low emissions analysis platform—integrated benefits calculator (LEAP-IBC) tool to assess air quality and climate co-benefits: application for Bangladesh *Environ. Int.* **145** 106155
- Laborte A G *et al* 2017 RiceAtlas, a spatial database of global rice calendars and production *Sci. Data.* **4** 170074
- Lassaletta L, Billen G, Garnier J, Bouwman L, Velazquez E, Mueller N D and Gerber J S 2016 Nitrogen use in the global food system: Past trends and future trajectories of agronomic performance, pollution, trade, and dietary demand *Environ. Res. Lett.* **11** 095007
- Lassaletta L, Billen G, Grizzetti B, Anglade J and Garnier J 2014 50 year trends in nitrogen use efficiency of world cropping systems: The relationship between yield and nitrogen input to cropland *Environ. Res. Lett.* **9** 105011
- Lelieveld J, Evans J S, Fnais M, Giannadaki D and Pozzer A 2015 The contribution of outdoor air pollution sources to premature mortality on a global scale *Nature* **525** 367
- Li C *et al* 2017 Trends in chemical composition of global and regional population-weighted fine particulate matter estimated for 25 Years *Environ. Sci. Technol.* **51** 11185–95
- Linnér B O, Mickwitz P and Román M 2012 Reducing greenhouse gas emissions through development policies: a framework for analysing policy interventions *Clim. Dev.* **4** 175–86
- Lloyd S J, Sari Kovats R and Chalabi Z 2011 Climate change, crop yields, and undernutrition: Development of a model to quantify the impact of climate scenarios on child undernutrition *Environ. Health Perspect.* **119** 1817–23
- McDuffie E E, Smith S J, O’Rourke P, Tibrewal K, Venkataraman C, Marais E A, Zheng B, Crippa M, Brauer M and Martin R V 2020 A global anthropogenic emission inventory of atmospheric pollutants from sector- and fuel-specific sources (1970–2017): an application of the Community Emissions Data System (CEDS). *Earth Syst Sci. Data* **12** 3413–42
- Mohankumar Sajeev E P, Winiwarter W and Amon B 2018 Greenhouse gas and ammonia emissions from different stages of liquid manure management chains: abatement options and emission interactions *J. Environ. Qual.* **47** 30–41
- Muhammad A, D’Souza A, Meade B, Micha R and Mozaffarian D 2017 How income and food prices influence global dietary intakes by age and sex: Evidence from 164 countries *BMJ Glob. Heal.* **15** e000184

- Murray C J L et al 2020 Global burden of 87 risk factors in 204 countries and territories, 1990–2019: a systematic analysis for the global burden of disease study 2019 *Lancet* **396** 1223–49
- Myhre G et al 2013 IPCC Fifth Assessment Report (AR5) *Anthropogenic and Natural Radiative Forcing. Clim. Chang. 2013 Phys. Sci. Basis.* (<https://doi.org/10.1017/CBO9781107415324.018>)
- Nault B A et al 2020 Anthropogenic secondary organic aerosols contribute substantially to air pollution mortality *Atmos. Chem. Phys. Discuss.* (<https://doi.org/10.5194/acp-2020-914>)
- O'Rourke P R, Smith S J, McDuffie E E, Crippa M, Klimont Z, Mott A, Wang S, Nicholson M B, Feng L and Hoesly R M 2020 (2020, September 11). CEDS v-2020-09-11 Pre-Release Emission Data 1975-2019 (Version Sept-11-2020) *Zenodo.* (<https://doi.org/10.5281/zenodo.4025316>)
- Olofin I et al 2013 Associations of suboptimal growth with all-cause and cause-specific mortality in children under five years: a pooled analysis of ten prospective studies *PLoS One* **29** e64636
- Paulot F, Jacob D J, Pinder R W, Bash J O, Travis K and Henze D K 2014 Ammonia emissions in the United States, European Union, and China derived by high-resolution inversion of ammonium wet deposition data: Interpretation with a new agricultural emissions inventory (MASAGE\_NH3) *J. Geophys. Res.* **119** 4343–64
- Pellegrini P and Fernández R J 2018 Crop intensification, land use, and on-farm energy-use efficiency during the worldwide spread of the green revolution *Proc. Natl. Acad. Sci. U. S. A.* **115** 2335–40
- Pinder R W, Adams P J, Pandis S N and Gilliland A B 2006 Temporally resolved ammonia emission inventories: Current estimates, evaluation tools, and measurement needs *J. Geophys. Res. Atmos.* **111**
- Qu Z, Henze D K, Cooper O R and Neu J L 2020 Impacts of global NO<sub>x</sub> inversions on NO<sub>2</sub> and ozone simulations *Atmos. Chem. Phys.* **20** 13109–30
- REVIHAAP 2013 Review of evidence on health aspects of air pollution—REVIHAAP Project technical report. World Health Organization (WHO) Regional Office for Europe. Bonn. Available: ([http://www.euro.who.int/\\_\\_data/assets/pdf\\_file/0004/193108/REVIHAAP-Final-technical-rep](http://www.euro.who.int/__data/assets/pdf_file/0004/193108/REVIHAAP-Final-technical-rep))
- Robinson T P et al 2011 *Global Livestock Production Systems* (Rome: Food and Agriculture Organization of the United Nations) p 152
- Ross K, Hite K, Waite R, Carter R, Pegorsch L, Damassa T and Gasper R 2019 NDC enhancement: opportunities in agriculture *World Resources Institute Report.* Available at: (<https://www.wri.org/publication/enhancing-ndcs-agriculture>)
- San Martín W 2020 Global Nitrogen in Sustainable Development: Four Challenges at the Interface of Science and Policy *Life on Land. Encyclopedia of the UN Sustainable Development Goals* (Cham: Springer) ([https://doi.org/10.1007/978-3-319-71065-5\\_114-1](https://doi.org/10.1007/978-3-319-71065-5_114-1))
- Shindell D, Borgford-Parnell N, Brauer M, Haines A, Kuylenstierna J C I, Leonard S A, Ramanathan V, Ravishankara A, Amann M and Srivastava L 2017 A climate policy pathway for near- and long-term benefits *Science* **356** 93–494
- Springmann M, Godfray H C J, Rayner M and Scarborough P 2016a Analysis and valuation of the health and climate change cobenefits of dietary change *Proc. Natl. Acad. Sci. U. S. A.* **113** 4146–51
- Springmann M, Mason-D'Croz D, Robinson S, Garnett T, Godfray H C J, Gollin D, Rayner M, Ballon P and Scarborough P 2016b Global and regional health effects of future food production under climate change: a modelling study *Lancet* **387** 1937–46
- Springmann M, Mason-D'Croz D, Robinson S, Wiebe K, Godfray H C J, Rayner M and Scarborough P 2017 Mitigation potential and global health impacts from emissions pricing of food commodities *Nat. Clim. Chang.* **7** 69–74
- Springmann M, Wiebe K, Mason-D'Croz D, Sulser T B, Rayner M and Scarborough P 2018 Health and nutritional aspects of sustainable diet strategies and their association with environmental impacts: a global modelling analysis with country-level detail *Lancet Planet. Heal.* **2** e451–e461
- Tilman D and Clark M 2014 Global diets link environmental sustainability and human health *Nature* **515** 518–22
- Tonini D, Albizzati P F and Astrup T F 2018 Environmental impacts of food waste: learnings and challenges from a case study on UK *Waste Manag.* **76** 744–66
- Turner Michelle C et al 2016 Long-Term Ozone Exposure and Mortality in a Large Prospective Study *Am. J. Respir. Crit. Care Med.* **193** 1134–42
- UNEP CCAC 2021 United Nations Environment Programme and Climate and Clean Air Coalition. Global Methane Assessment: Benefits and Costs of Mitigating Methane Emissions. Nairobi: United Nations Environment Programme. ISBN: 978-92-807-3854-4 (<https://www.ccaoalition.org/en/resources/global-methane-assessment-full-report>)
- United Nations Department of Economic and Social Affairs Population Division 2019 World population prospects 2019, Department of Economic and Social Affairs *World Population Prospects 2019*
- Walling E and Vaneekhaute C 2020 Greenhouse gas emissions from inorganic and organic fertilizer production and use: A review of emission factors and their variability *J. Environ. Manage.* **276** 111211
- Wang C, Yin S, Bai L, Zhang X, Gu X, Zhang H, Lu Q and Zhang R 2018 High-resolution ammonia emission inventories with comprehensive analysis and evaluation in Henan, China, 2006–2016 *Atmos. Environ.* **193** 11–23
- Warner J X, Wei Z, Larrabee Strow L, Dickerson R R and Nowak J B 2016 The global tropospheric ammonia distribution as seen in the 13-year AIRS measurement record *Atmos. Chem. Phys.* **16** 5467–79
- Wendt A S, Sparling T M, Waid J L, Mueller A A and Gabrysch S 2019 Food and agricultural approaches to reducing malnutrition (FAARM): protocol for a cluster-randomised controlled trial to evaluate the impact of a homestead food production programme on undernutrition in rural Bangladesh *BMJ Open* **9** 1–11
- WHO 2015 WHO estimates of the global burden of foodborne diseases *World Health Organisation Report.* Available at: (<https://www.who.int/publications/i/item/9789241565165>)
- Willett W et al 2019 Food in the anthropocene: the EAT–Lancet commission on healthy diets from sustainable food systems *Lancet* **393** 447–92
- Yevich R and Logan J A 2003 An assessment of biofuel use and burning of agricultural waste in the developing world *Global Biogeochem. Cycles* **17** 1095
- Yip C S C, Lam W and Fielding R 2018 A summary of meat intakes and health burdens *Eur. J. Clin. Nutr.* **72** 18–29
- Yu Q, You L, Wood-Sichra U, Ru Y, Joglekar A, Fritz S, Xiong W, Lu M, Wu W and Yang P 2020 A cultivated planet in 2010: 2. the global gridded agricultural production maps *Earth Syst. Sci.* **12** 3545–72
- Zagmutt F J, Pouzou J G and Costard S 2019 The EAT–Lancet Commission: a flawed approach? *Lancet* **394** 1140–1
- Zhang Q et al 2017 Transboundary health impacts of transported global air pollution and international trade *Nature* **543** 705–9
- Zimmermann R, Brüntrup M, Kolavalli S and Flaherty K 2009 Agricultural policies in Sub-Saharan Africa: understanding CAADP and APRM policy processes, Studies, No. 48, ISBN 978-3-88985-484-1, Deutsches Institut für Entwicklungspolitik (DIE), Bonn